Supporting Information

Near-Ambient Temperature Spin Crossover Controlled *via* the Self-Assembly of Chiral and Racemic Polymorphs in Triazolylimine [Fe$_2$L$_3$](BF$_4$)$_4$ Helicates

James P. Flood,† Matthew J. Wallis,† Joseph Tadros,† Yuto Nakashima,‡ Daniel J. Fanna,‖ Janice R. Aldrich-Wright,† Leonard F. Lindoy,§ Shinya Hayami,‡ and Feng Li*,†

†Western Sydney University, School of Science, Locked Bag 1797, Penrith, NSW, 2571, Australia.

‡Kumamoto University, Department of Chemistry, Graduate School of Science and Technology, 2-39-1 Kurokami, Chuo-ku, Japan.
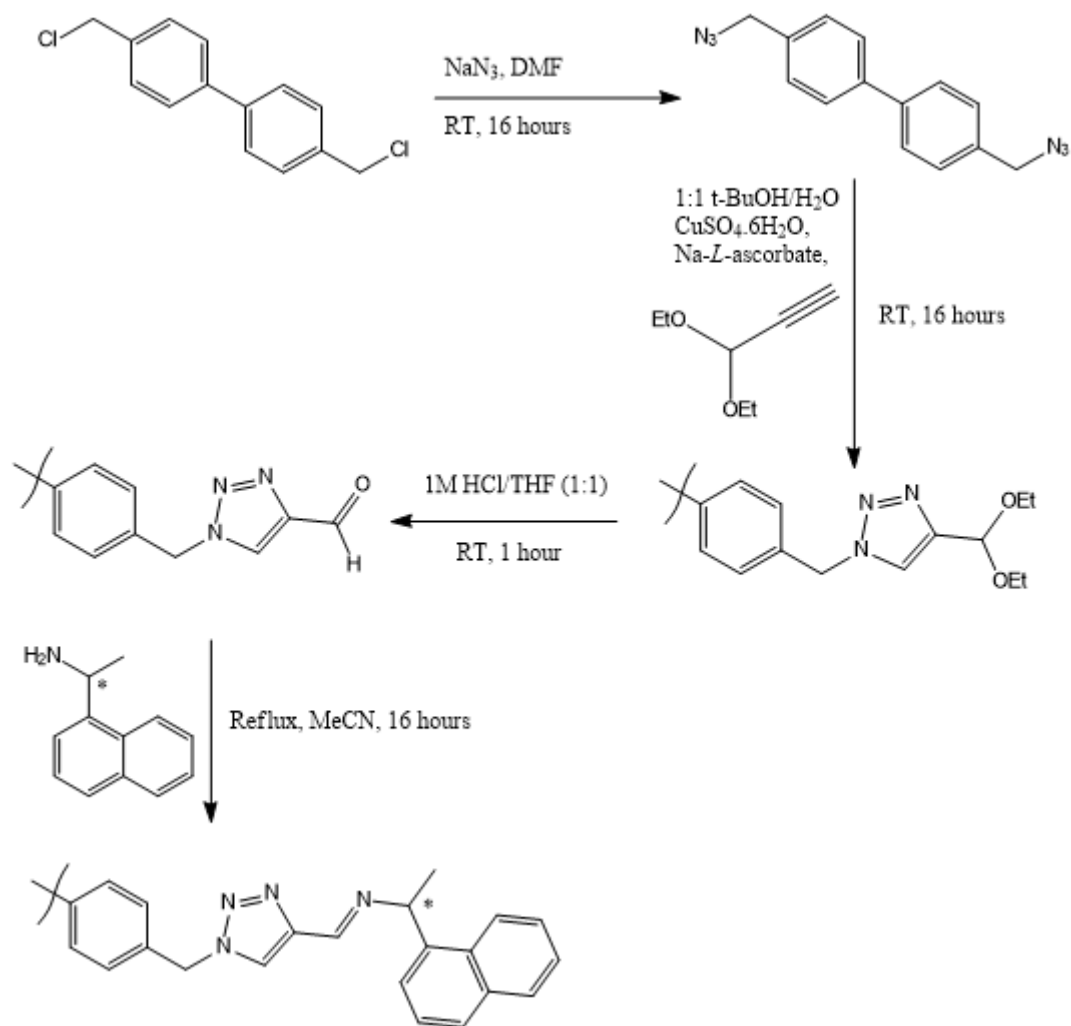
‖Western Sydney University, Advanced Materials Characterisation Facility, Locked Bag 1797, Penrith, NSW, Australia.

§The University of Sydney, School of Chemistry, NSW 2006, Australia.
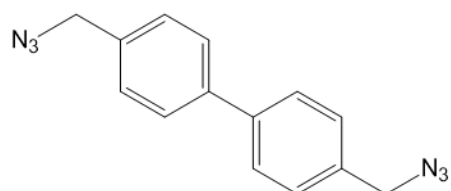
Table of Contents

Experimental

Scheme S1. The synthetic strategy to generate the reported C_2-symmetric bis-bidentate ligand, **L**.

4,4'-Bis(azidomethyl)-1,1'-biphenyl

4,4'-Bis(azidomethyl)-1,1'-biphenyl was obtained using a previously reported method.[1] NaN$_3$ (5.0 g, 76.9 mmol) was added to a stirred solution of 4,4'-bis(chloromethyl)-1,1'-biphenyl (9.6 g, 38.2 mmol) in DMF (50 mL) and stirring was continued at room temperature overnight. The solution was then added to a beaker of vigorously stirred ice-cold water (150 mL). The desired 4,4'-bis(azidomethyl)-1,1'-biphenyl precipitated out of the stirred solution immediately. The precipitate was collected by vacuum filtration and washed with cold water (3 x 50 mL) to afford the product as a white amorphous powder (10.0 g, 98%). ^{1}H NMR (DMSO-d$_6$, 400 MHz) δ 7.73 (d, J = 8.0 Hz, 4H), 7.47 (d, J = 7.9 Hz, 4H), 4.50 (s, 4H). ^{13}C NMR (DMSO-d$_6$, 101 MHz) δ 139.40, 135.01, 129.13, 127.02, 53.28.
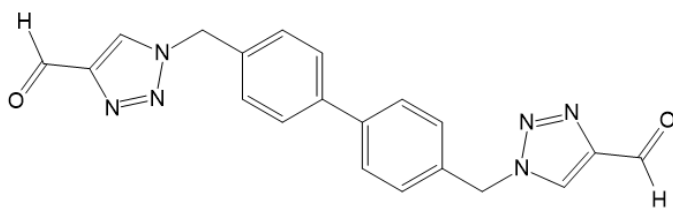
4,4'-Bis(4-(diethoxymethyl)-1H-1,2,3-triazol-1-yl)methyl)-1,1'-biphenyl
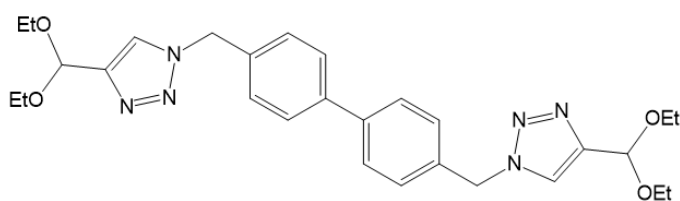
CuSO$_4$.5H$_2$O (47 mg, 0.188 mmol,), sodium-*L*-ascorbate (75 mg, 0.379 mmol), and propargylaldehyde diethyl acetal (1.1 mL, 7.568 mmol) were added sequentially to a vigorously stirred solution of 4,4'-bis(azidomethyl)-1,1'-biphenyl (1.0 g, 3.784 mmol) in 1:1 *t*-BuOH:H$_2$O (30 mL) and the reaction solution was stirred at room temperature overnight. The precipitated solid was then collected by vacuum filtration and washed with cold water (3 x 20 mL), affording the product as a green-white powder (1.9 g, 94%). ^{1}H NMR (400 MHz, DMSO-d$_6$) δ 8.16 (s, 2H), 7.67 (d, *J* = 8.1 Hz, 4H), 7.40 (d, *J* = 8.1 Hz, 4H), 5.63 (d, 6H), 4.50 (d, 2H), 3.54 (m, 9H), 1.12 (t, 13H). ^{13}C NMR (DMSO-d$_6$, 101 MHz) δ 139.84, 135.84, 129.53, 129.24, 127.54, 123.67, 96.63, 61.15, 52.09, 15.54. ESI-HRMS (positive ion detection, MeCN *m/z*): calculated for [M + Na]$^+$: 543.2696, Found: 543.4076.
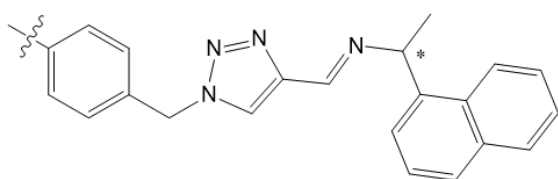
1,1'-([1,1'-Biphenyl]-4,4'-diylbis(methylene))bis(1H-1,2,3-triazole-4-carbaldehyde)

Excess 1M HCl (30 mL) was added to a stirred solution of 4,4'-bis(4-(diethoxymethyl)-1H-1,2,3-triazol-1-yl)methyl)-1,1'-biphenyl (1.9 g, 3.649 mmol) in THF (30 mL) and the reaction was stirred at room temperature for one hour. The precipitated solid that formed was collected by vacuum filtration and washed with cold water (3 x 30 mL), affording the product as an off-white powder (1.3 g, 98%). ^{1}H NMR (DMSO-d$_6$, 400 MHz) δ 10.01 (s, 2H), 8.99 (s, 2H), 7.67 (d, *J* = 8.0 Hz, 4H), 7.45 (d, *J* = 8.0 Hz, 4H), 5.74 (s, 4H). ^{13}C NMR (DMSO-d$_6$, 101 MHz) δ 185.24, 147.35, 139.84, 134.98, 129.08, 128.64, 127.47, 53.16. ESI-HRMS (ESI$^+$, *m/z*): calculated for [M + Na]$^+$: 395.1232, Found: 395.2156.

Reaction of 1,1'-([1,1'-biphenyl]-4,4'-diylbis(methylene))bis(1H-1,2,3-triazole-4-carbaldehyde) with R-NH$_2$ derivatives

1,1'-([1,1'-Biphenyl]-4,4'-diylbis(methylene))bis(1H-1,2,3-triazole-4-carbalde-hyde) (500 mg, 1.343 mmol) in MeCN (50 mL) was added to a 100 mL round bottom flask and the resulting suspension was heated at reflux for 30 minutes. The appropriate 1-(1-naphthyl)ethylamine substrate (489 mg, 2.856 mmol) was added in one portion and the homogenous solution was heated at reflux

overnight. The resulting precipitate was isolated by vacuum filtration and washed with cold MeCN (3 x 10 mL) to afford the solid imine products as a brown-white or off-white powder.

(N,N'E,N,N'E)-N,N'-((1,1'-([1,1'-biphenyl]-4,4'-diylbis(methylene))bis(1H-1,2,3-triazole-4,1-diyl))bis(methanylylidene))bis(1-(naphthalen-1-yl)ethanamine) (*rac*-L)

Yield: 25.2% ^{1}H NMR (DMSO-d[6], 400 MHz) δ 8.67 (s, 1H), 8.65 (s, 1H), 8.26 (d, *J* = 8.3 Hz, 1H), 7.94 (d, *J* = 7.8 Hz, 1H), 7.83 (d, *J* = 8.2 Hz, 1H), 7.74 (d, *J* = 6.7 Hz, 1H), 7.64 (d, *J* = 8.3 Hz, 2H), 7.52 (ddd, *J* = 19.4, 9.8, 2.6 Hz, 3H), 7.43 (d, *J* = 8.3 Hz, 2H), 5.66 (s, 2H), 5.44 (q, *J* = 6.5 Hz, 1H), 1.60 (d, *J* = 6.6 Hz, 3H). ^{13}C NMR (DMSO-d[6], 101 MHz) δ 152.54, 146.31, 140.95, 139.95, 135.52, 133.98, 130.72, 129.20, 127.68, 127.59, 126.52, 126.05, 125.97, 124.72, 124.17, 123.92, 118.55, 64.69, 53.17, 24.61. ESI-HRMS (ESI[+], *m/z*): calculated for [M + Na][+]: 701.3117, Found: 701.4924.

(1E,1'E)-1,1'-((1,1'-biphenyl-4,4'-diylbis(methylene))bis(1H-1,2,3-triazole-1,4-diyl))bis(N-((*R*)-1-napthalen-1-yl)methanimine) (*R*-L)

Yield: 18.9% ^{1}H NMR (DMSO-d[6], 400 MHz) δ 8.67 (s, 1H), 8.64 (s, 1H), 8.26 (d, *J* = 8.4 Hz, 1H), 7.94 (d, *J* = 8.0 Hz, 1H), 7.83 (d, *J* = 8.2 Hz, 1H), 7.74 (d, *J* = 6.7 Hz, 1H), 7.64 (d, *J* = 8.3 Hz, 2H), 7.52 (ddd, *J* = 19.5, 8.2, 3.9 Hz, 3H), 7.43 (d, *J* = 8.3 Hz, 2H), 5.66 (s, 2H), 5.44 (q, *J* = 6.5 Hz, 1H), 1.60 (d, *J* = 6.6 Hz, 3H). ^{13}C NMR (DMSO-d[6], 101 MHz) δ 152.55, 146.30, 140.95, 139.95, 135.53, 133.98, 130.72, 129.20, 127.69, 127.59, 126.53, 126.06, 125.98, 124.74, 124.18, 123.93, 64.68, 53.16, 24.62. ESI-HRMS (ESI[+], *m/z*): calculated for [M + H][+]: 679.3298, Found: 679.5107.

(1E,1'E)-1,1'-((1,1'-biphenyl-4,4'-diylbis(methylene))bis(1H-1,2,3-triazole-1,4-diyl))bis(N-((*S*)-1-napthalen-1-yl)methanimine) (*S*-L)

Yield: 16.4% ^{1}H NMR (DMSO-d[6], 400 MHz) δ 8.68 (s, 1H), 7.93 (d, *J* = 7.9 Hz, 1H), 7.82 (d, *J* = 8.2 Hz, 1H), 7.74 (d, *J* = 7.2 Hz, 1H), 7.64 (d, *J* = 7.9 Hz, 2H), 7.52 (ddd, *J* = 19.2, 9.8, 4.6 Hz, 3H), 7.43 (d, *J* = 7.9 Hz, 2H), 5.65 (s, 2H), 5.44 (q, *J* = 6.6 Hz, 1H), 1.60 (d, *J* = 6.5 Hz, 3H). ^{13}C NMR (DMSO-d[6], 101 MHz) δ 152.08, 145.86, 140.53, 139.48, 135.08, 133.52, 130.26, 128.72, 127.20, 127.12, 126.03, 125.58, 125.49, 124.26, 123.70, 123.48, 64.23, 52.69, 24.20. ESI-HRMS (ESI[+], *m/z*): calculated for [M + H][+]: 697.3298, Found: 679.4941.

Complexation of the L analogs

Fe(BF$_4$)$_2$·6H$_2$O (224 mg, 0.664 mmol) in MeCN (10 mL) was added dropwise to a suspension of the appropriate **L** derivative (300 mg, 0.442 mmol) in MeCN (20 mL). This mixture was heated at reflux under a N$_2$ atmosphere for 1 hour resulting in a dark red solution. This solution was filtered hot and diethyl ether was allowed to diffuse into the solution over 48 hours leading to formation of the respective analogs of **1** as dark red rod-like crystals.

Λ-1

Yield 70.7%. ESI-HRMS (ESI$^+$, *m/z*): calculated for $[Fe_2L_3]^{4+}$: 536.9602, Found: 536.9463. TGA, 3.32% mass lost. Elemental analysis: Experimental, C (61.56), H (4.62), N (13.15); Calculated (for $[Fe_2L_3](BF_4)_4 + 4.75\ H_2O$), C (61.43), H (4.82), N (13.02)%. FTIR (cm^{-1}): 3137, 3060, 2971 (Ar. C-H), 1693 (Imine C=N). CD (λ (nm), MeCN): 540 (-16.33), 469 (+10.07), 413 (+15.22), 362 (-15.78).

Λ-1

Yield 47.3%. ESI-HRMS (ESI$^+$, *m/z*): calculated for $[Fe_2L_3]^{4+}$: 536.9602, Found: 536.9463. TGA, 2.39% mass lost. Elemental analysis: Experimental, C (61.78), H (4.68), N (13.09); Calculated (for $[Fe_2L_3](BF_4)_4 + 3.5\ H_2O$), C (61.97), H (4.77), N (13.14)%. FTIR (cm^{-1}): 3137, 3061, 2971, 2938 (Ar. C-H), 2349 (Triazole-N$_3$), 1697 (Imine C=N). CD (λ (nm), MeCN): 542 (+36.54), 472 (-24.15), 416 (-37.31), 364 (+39.58).

rac-**1**

Yield 5.0%. ESI-HRMS (ESI$^+$, *m/z*): calculated for $[Fe_2L_3]^{4+}$: 536.9602, Found: 536.6821. TGA, 3.04% mass lost. Elemental analysis: Experimental, C (61.62), H (4.72), N (12.83); Calculated (for $[Fe_2L_3](BF_4)_4 + 4.25\ H_2O$), C (61.64), H (4.80), N (13.07)%. FTIR (cm^{-1}): 3128, 3067, 2979, 2936 (Ar. C-H), 2250 (Triazole N$_3$), 1613 (Imine C=N).

Note: The yield for each analog was calculated from the mass of crystallites obtained *via* diffusion.
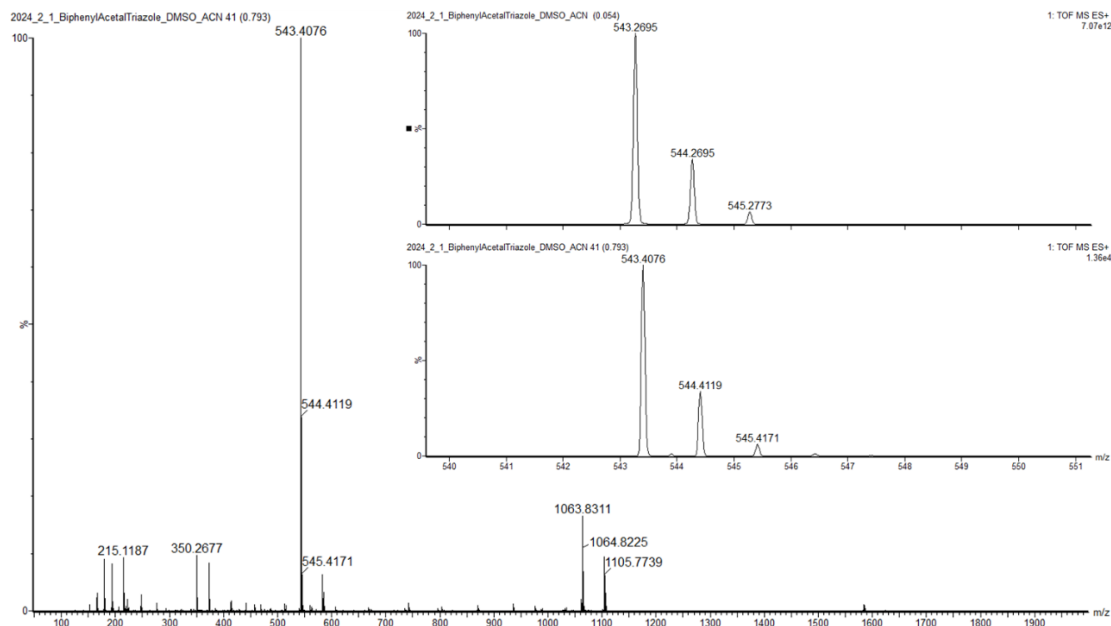
ESI-HRMS

Figure S1: ESI-HRMS of 4,4'-bis(4-(diethoxymethyl)-1H-1,2,3-triazol-1-yl)methyl)-1,1'-biphenyl. Inset shows the calculated (top) and experimental (bottom) isotope patterns for [M + Na]$^+$.
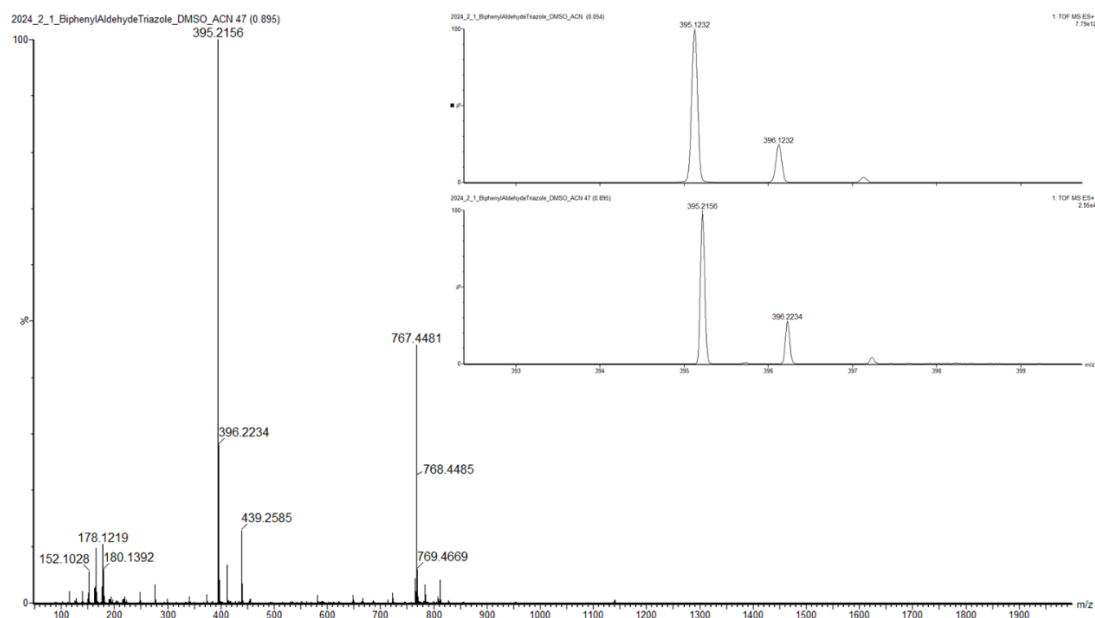

Figure S2: ESI-HRMS of 1,1'-([1,1'-biphenyl]-4,4'-diylbis(methylene))bis(1H-1,2,3-triazole-4-carbaldehyde). Inset shows the calculated (top) and experimental (bottom) isotope patterns for [M + Na]$^+$.
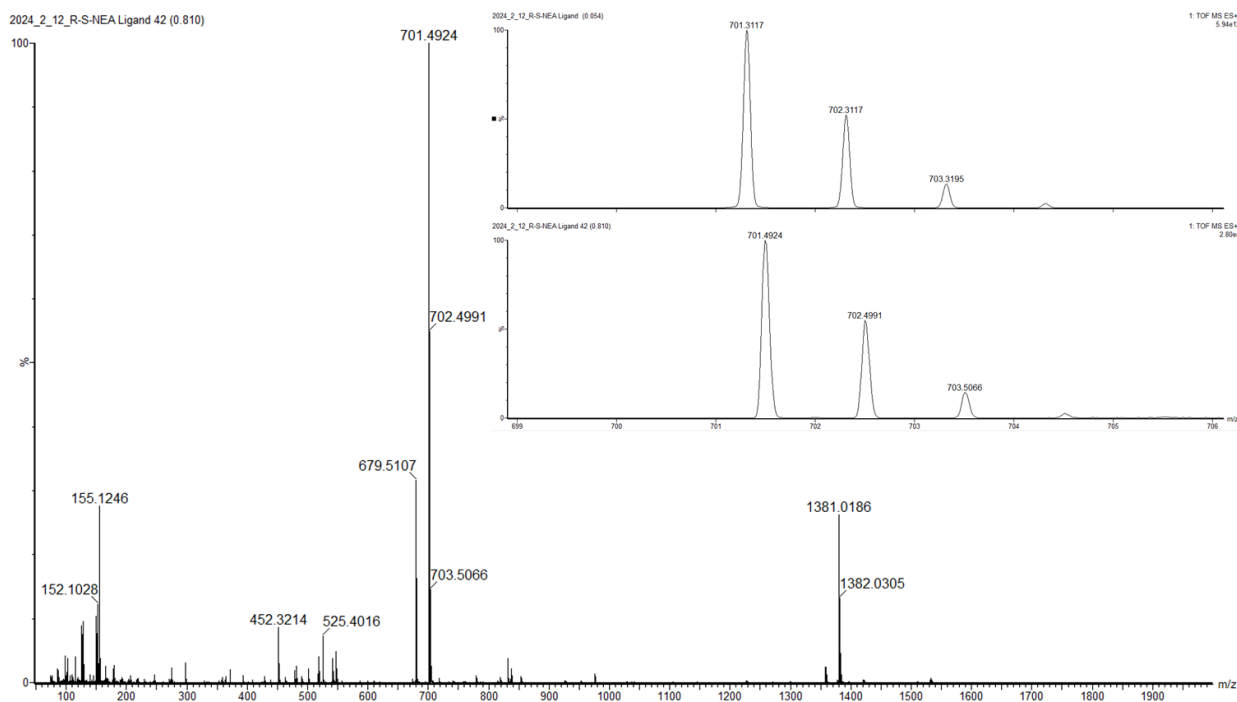
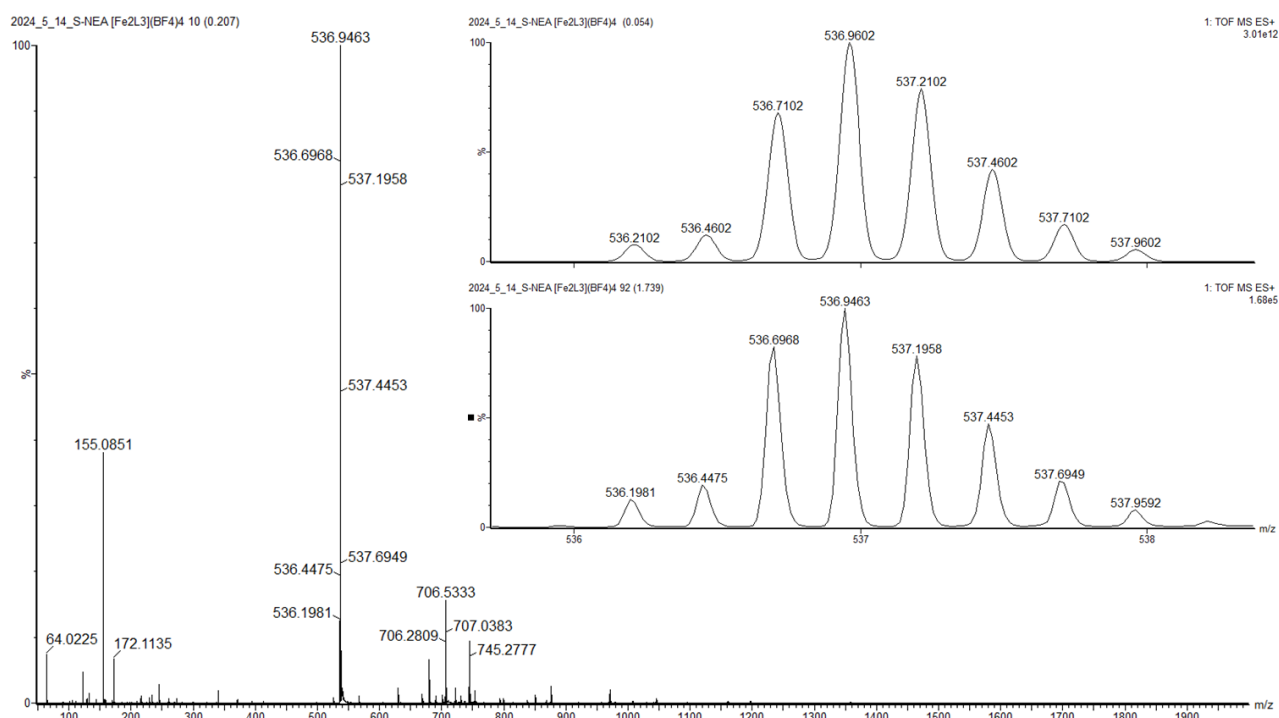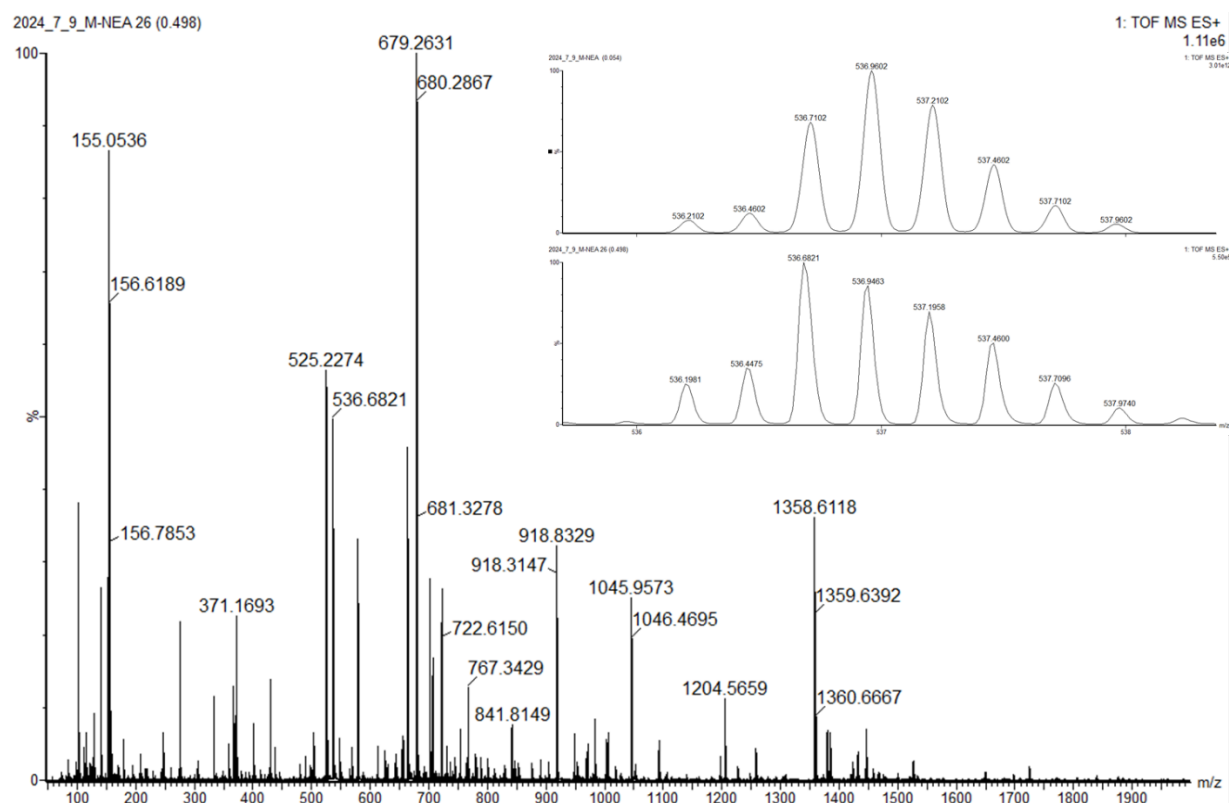**Figure S3**: ESI-HRMS of *rac*-**L**. Inset shows the calculated (top) and experimental (bottom) isotope patterns for [M + Na]⁺.
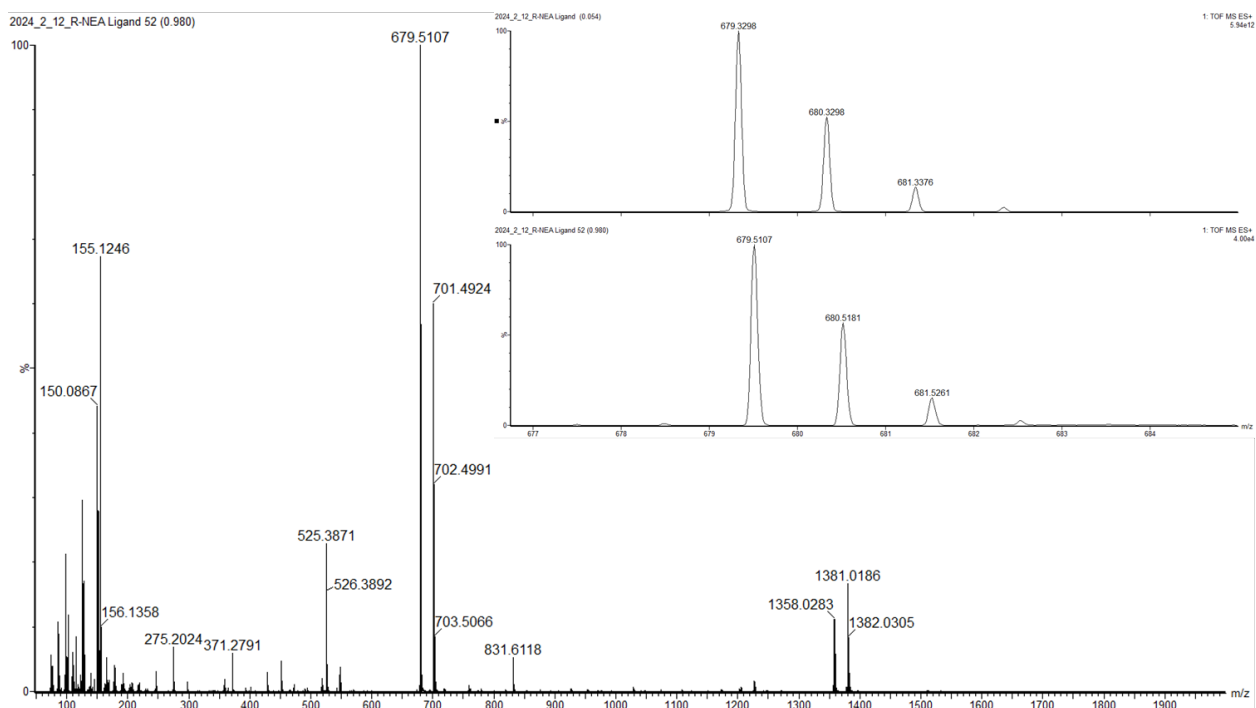
Figure S4: ESI-HRMS of *R*-**L**. Inset shows the calculated (top) and experimental (bottom) isotope patterns for [M + H]⁺.
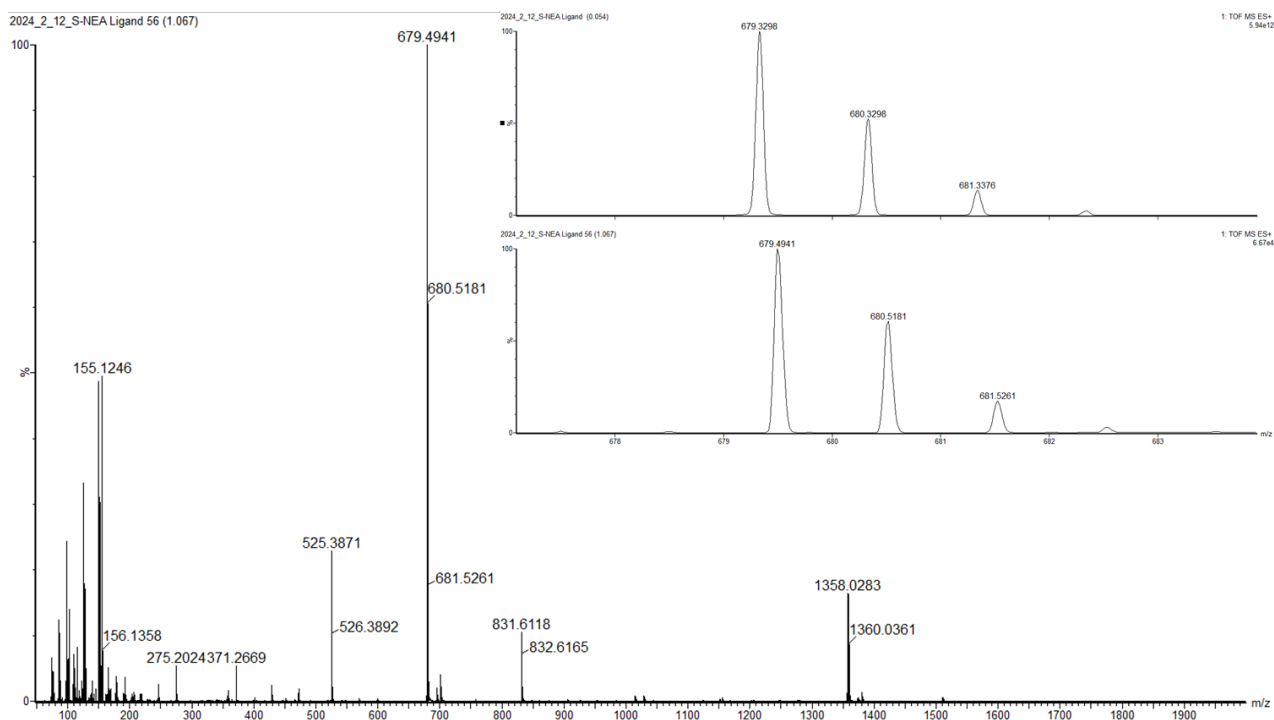
Figure S5: ESI-HRMS of *S*-**L**. Inset shows the calculated (top) and experimental (bottom) isotope patterns for [M + H]⁺.
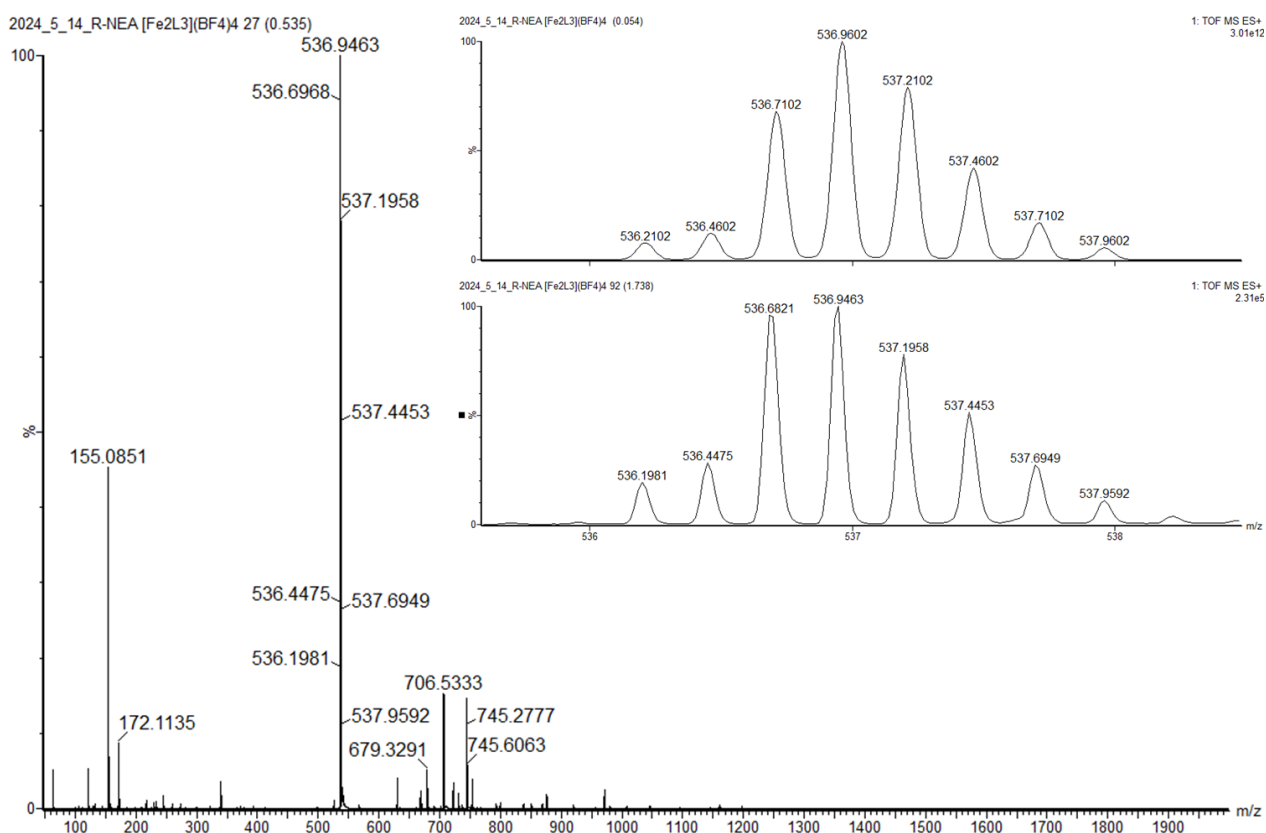
Figure S6: ESI-HRMS of Δ-**1**. Inset shows the calculated (top) and experimental (bottom) isotope patterns for [Fe**L**]⁴⁺.

Figure S7: ESI-HRMS of Λ-**1**. Inset shows the calculated (top) and experimental (bottom) isotope patterns for [Fe**L**]$^{4+}$.

Figure S8: ESI-HRMS of *rac*-**1**. Inset shows the calculated (top) and experimental (bottom) isotope patterns for [Fe**L**]$^{4+}$.

NMR
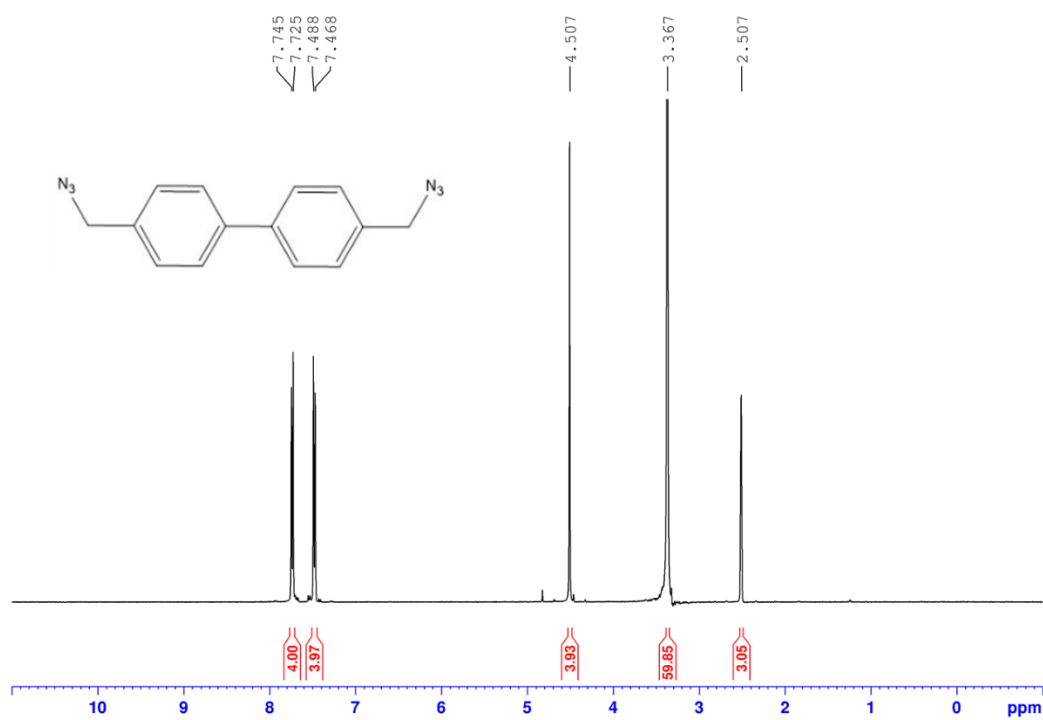
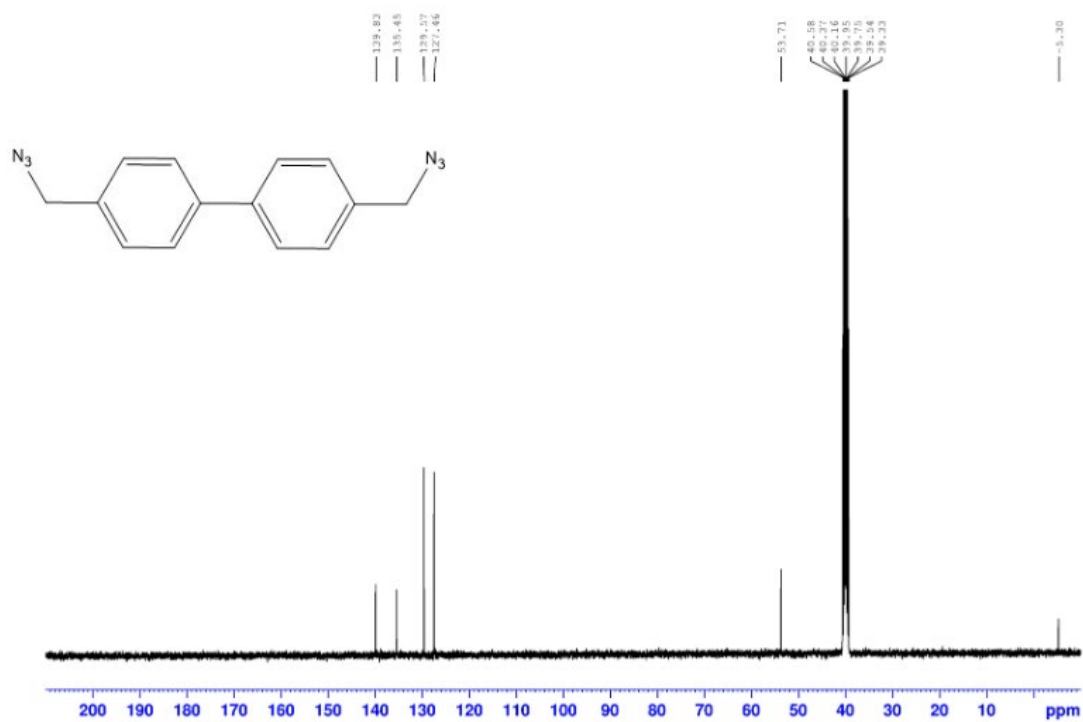**Figure S9**: ^{1}H NMR of 4,4'-bis(azidomethyl)-1,1'-biphenyl in DMSO-d^6.

Figure S10: ^{13}C NMR of 4,4'-bis(azidomethyl)-1,1'-biphenyl in DMSO-d^6.

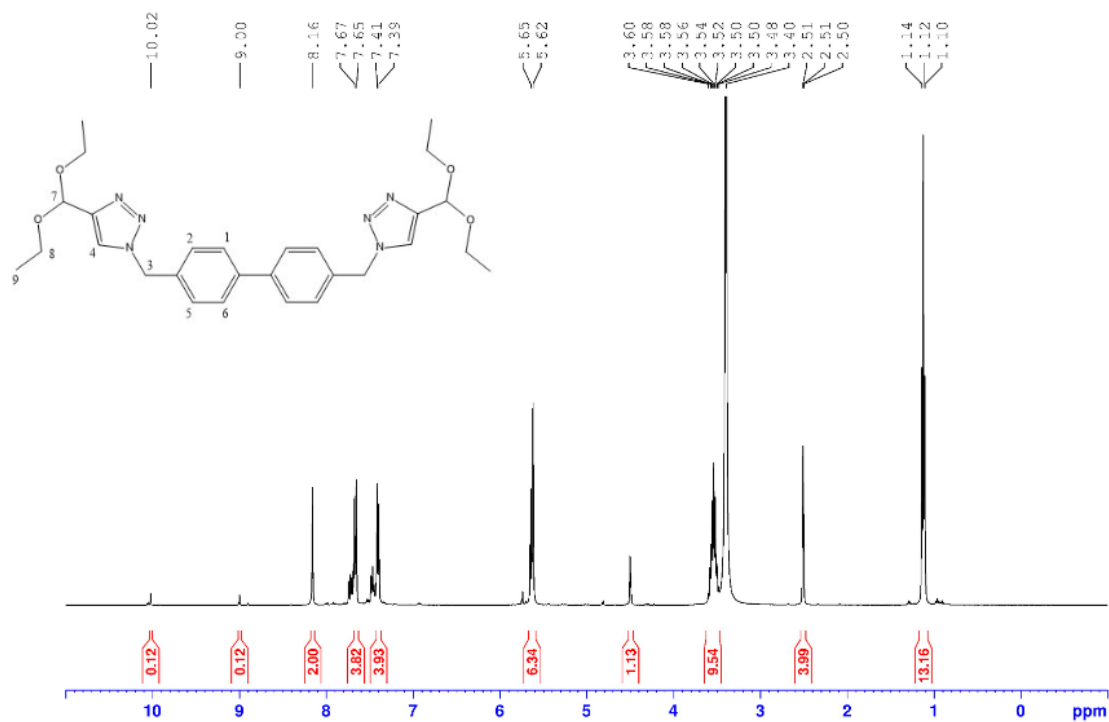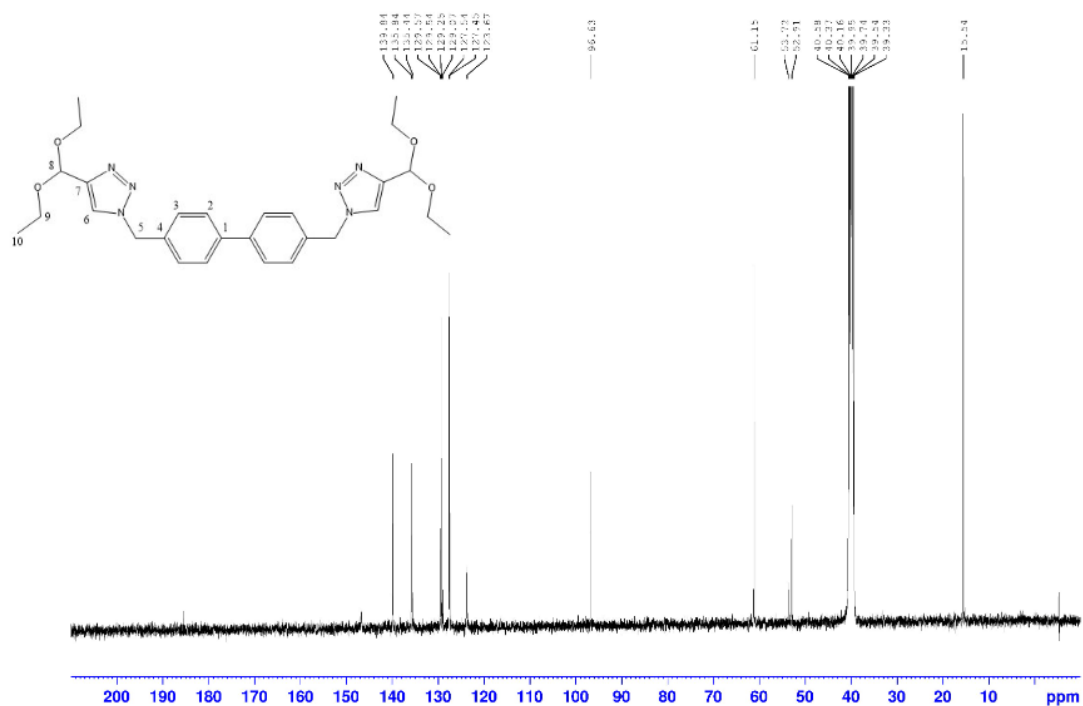**Figure S11**: ^{1}H NMR of 4,4'-bis(4-(diethoxymethyl)-1H-1,2,3-triazol-1-yl)methyl)-1,1'-biphenyl in DMSO-d[6].

Figure S12: ^{13}C NMR of 4,4'-bis(4-(diethoxymethyl)-1H-1,2,3-triazol-1-yl)methyl)-1,1'-biphenyl in DMSO-d[6].
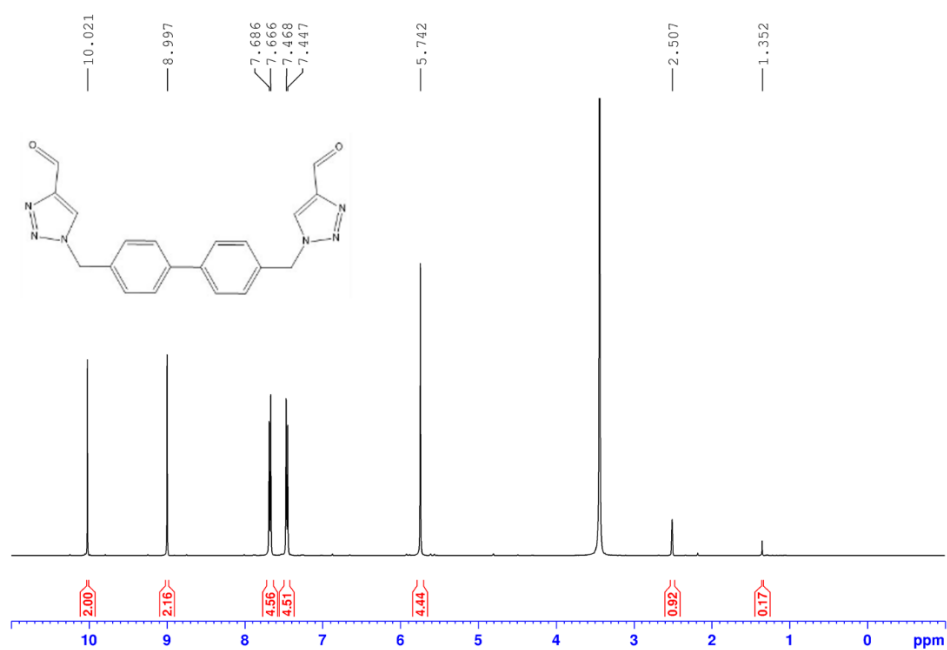
Figure S13: ^{1}H NMR of 1,1'-([1,1'-biphenyl]-4,4'-diylbis(methylene))bis(1H-1,2,3-triazole-4-carbaldehyde) in DMSO-d[6].
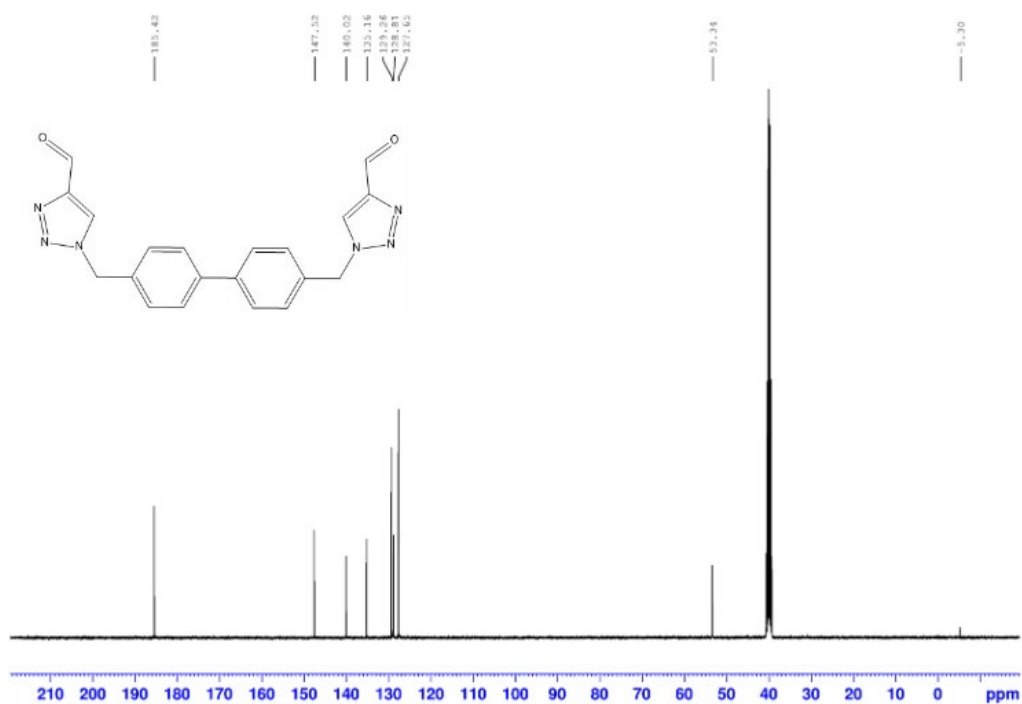

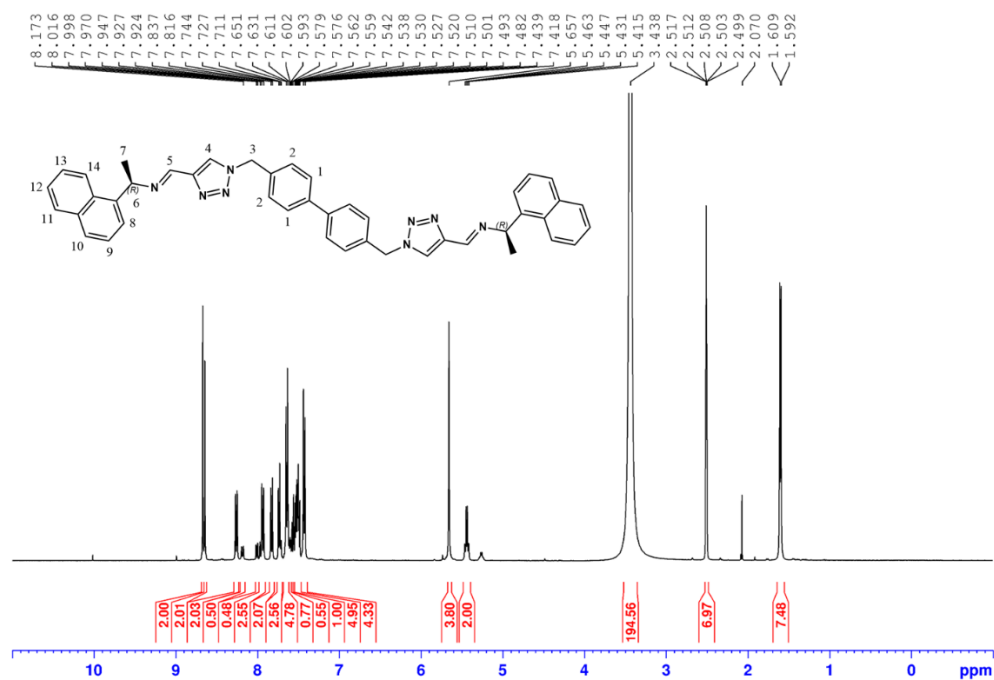**Figure S14**: ^{13}C NMR of 1,1'-([1,1'-biphenyl]-4,4'-diylbis(methylene))bis(1H-1,2,3-triazole-4-carbaldehyde) in DMSO-d[6].
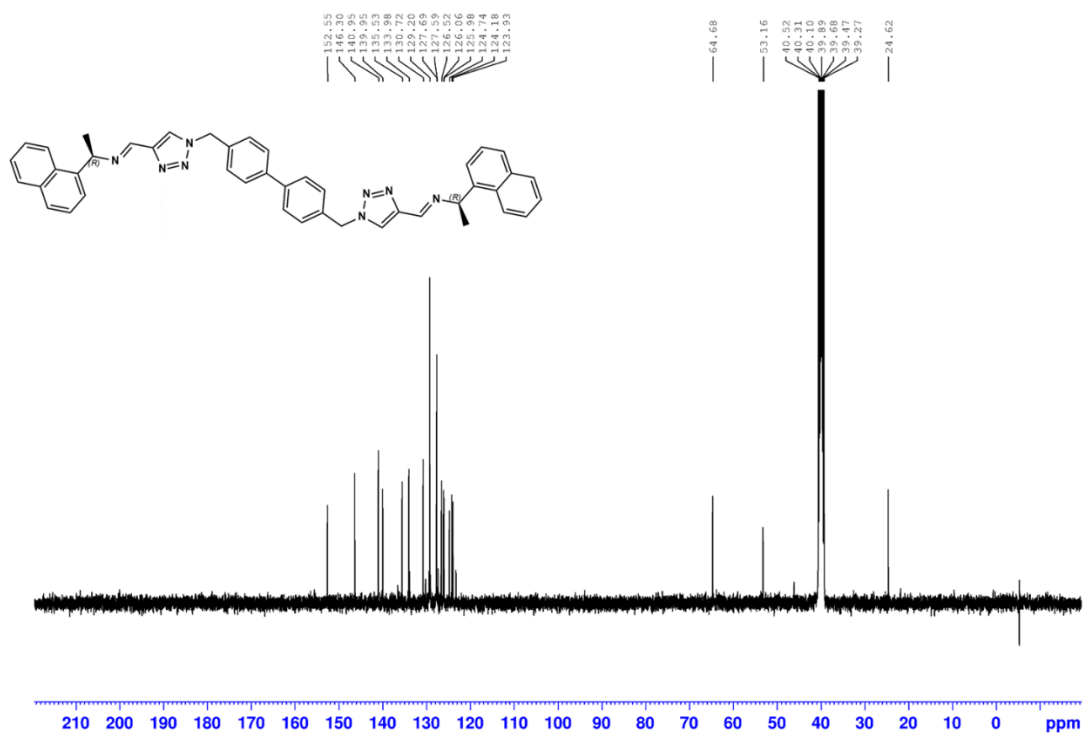
Figure S15: ^{1}H NMR of *R*-**L** in DMSO-d^6.
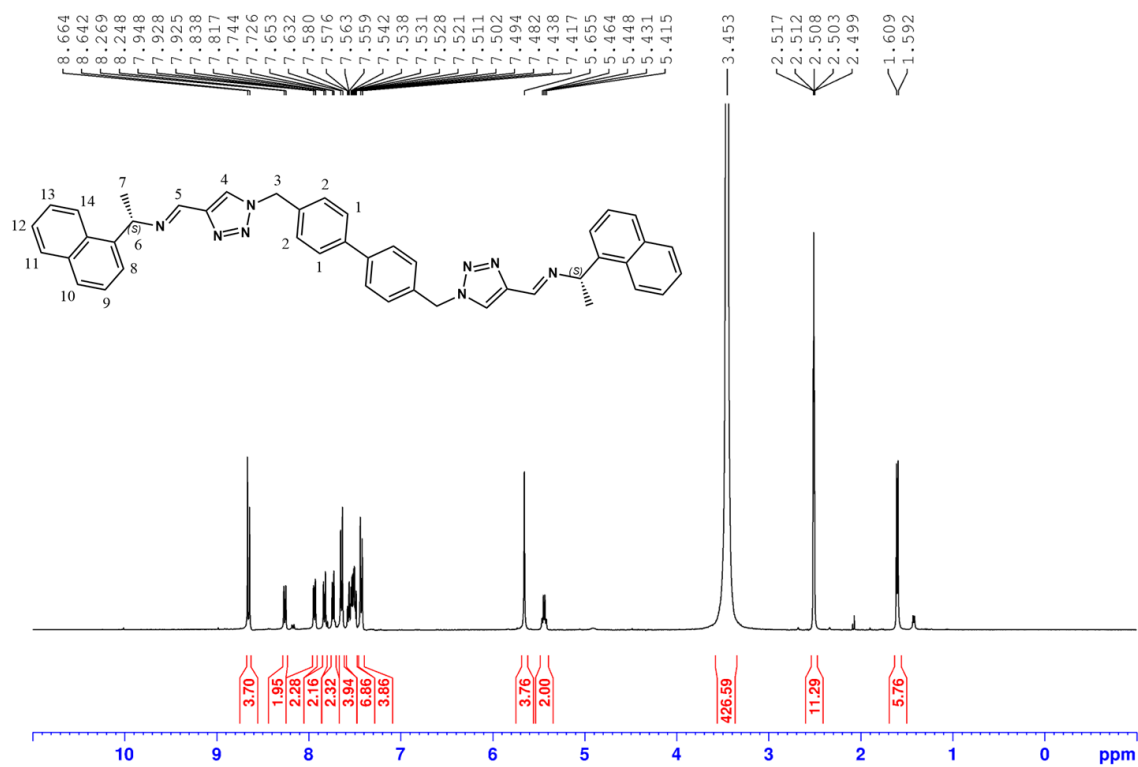

Figure S16: ^{13}C NMR of *R*-**L** in DMSO-d^6.

Figure S17: ^{1}H NMR of *S*-**L** in DMSO-d^6.
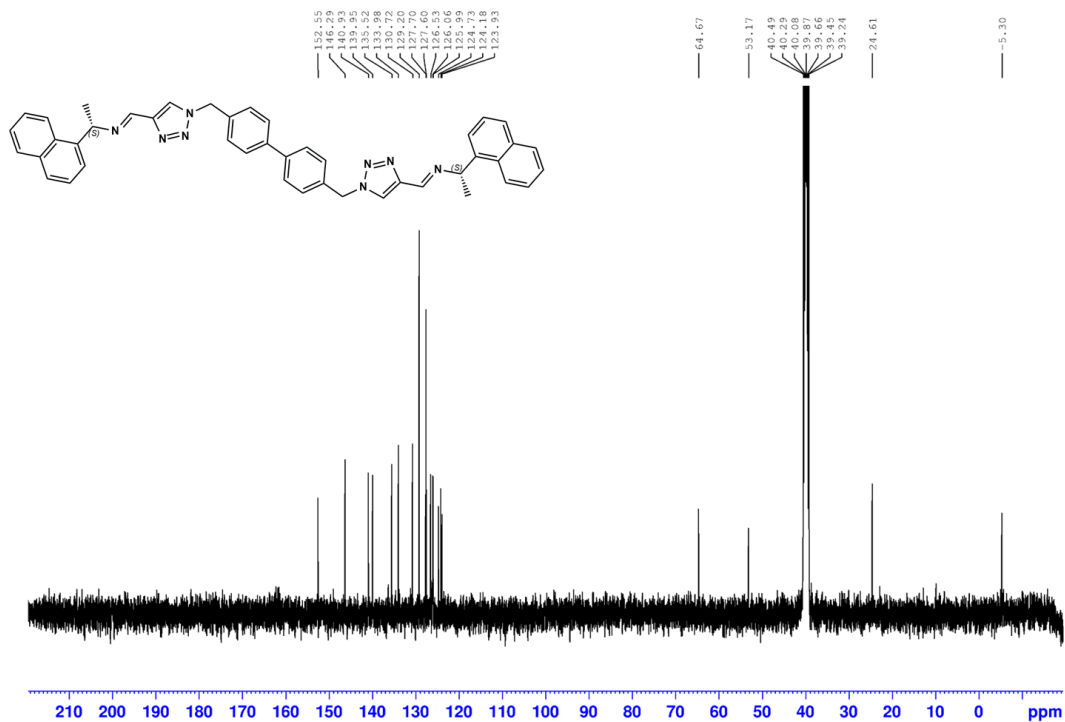
Figure S18: ^{13}C NMR of *S*-**L** in DMSO-d^6.
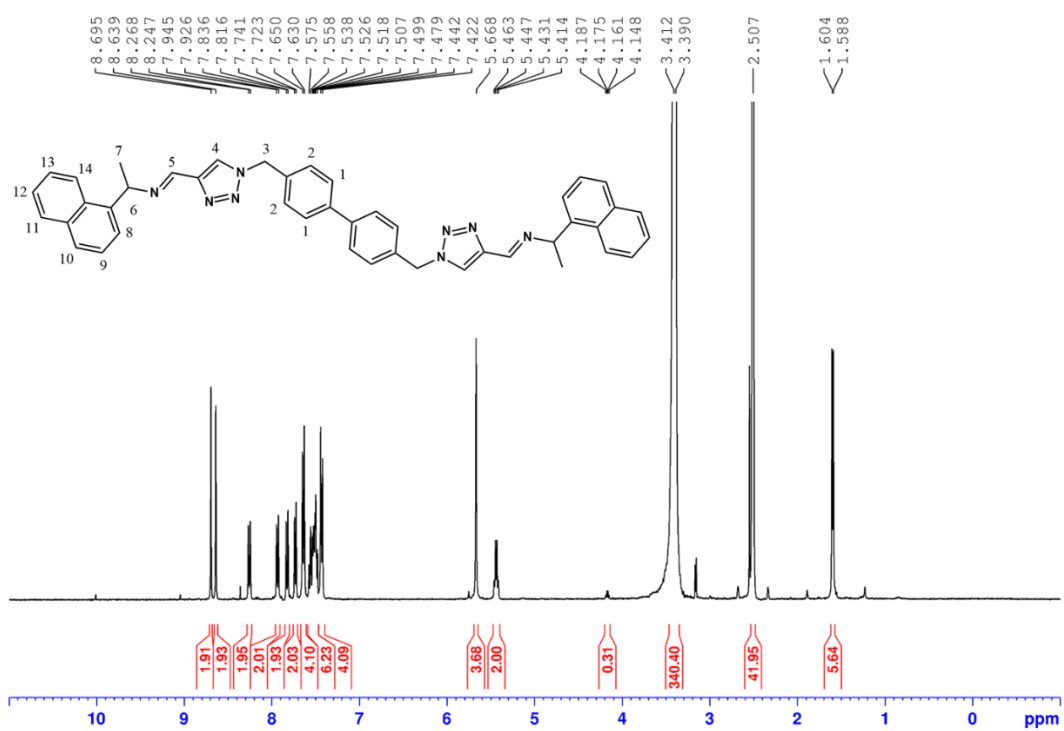
Figure S19: ^{1}H NMR of *rac*-**L** in DMSO-d^6.
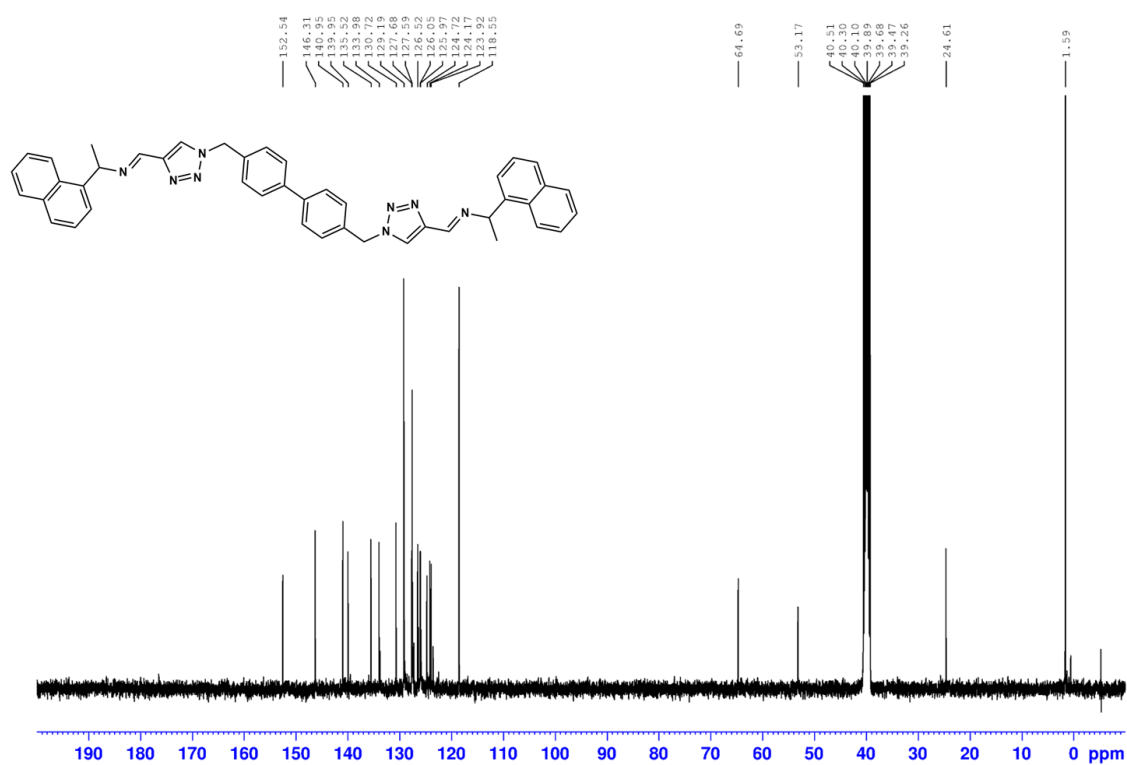
Figure S20: ^{13}C NMR of *rac*-**L** in DMSO-d^6.

FT-IR
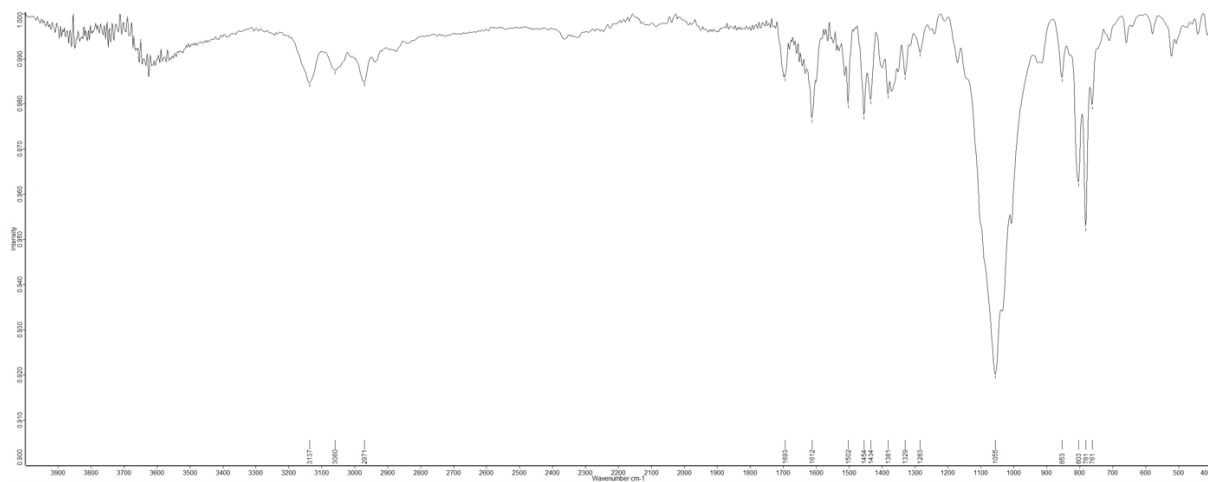
Figure S21: FT-IR of Δ-**1**.
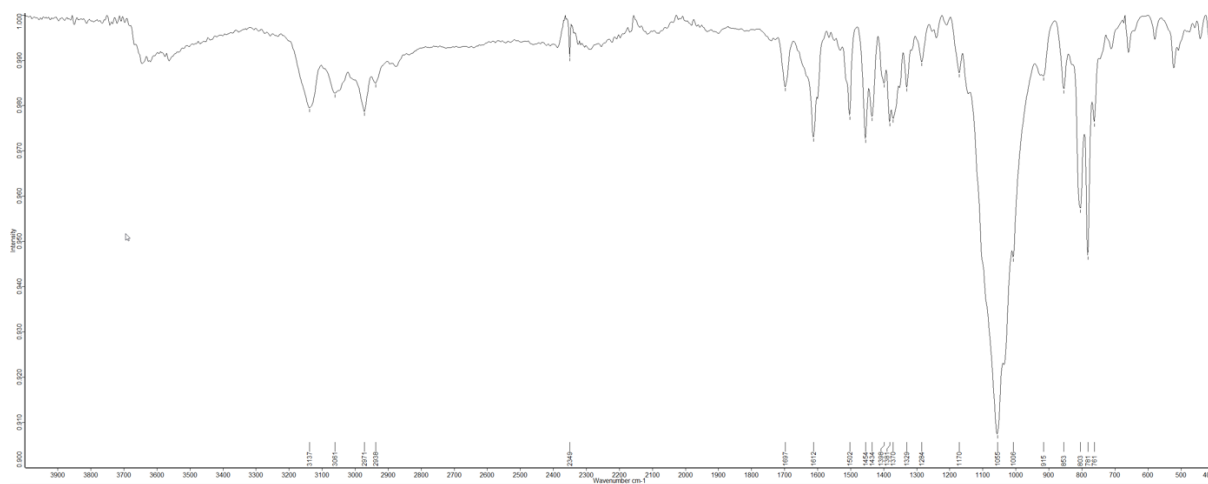
Figure S22: FT-IR of Λ-**1**.
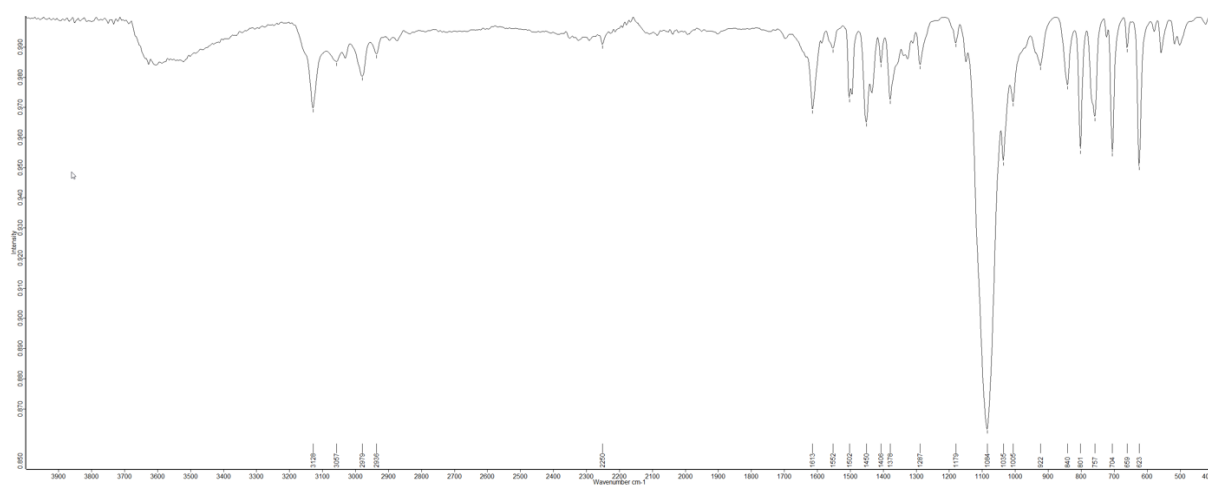
Figure S23: FT-IR of *rac*-**1**.

CD
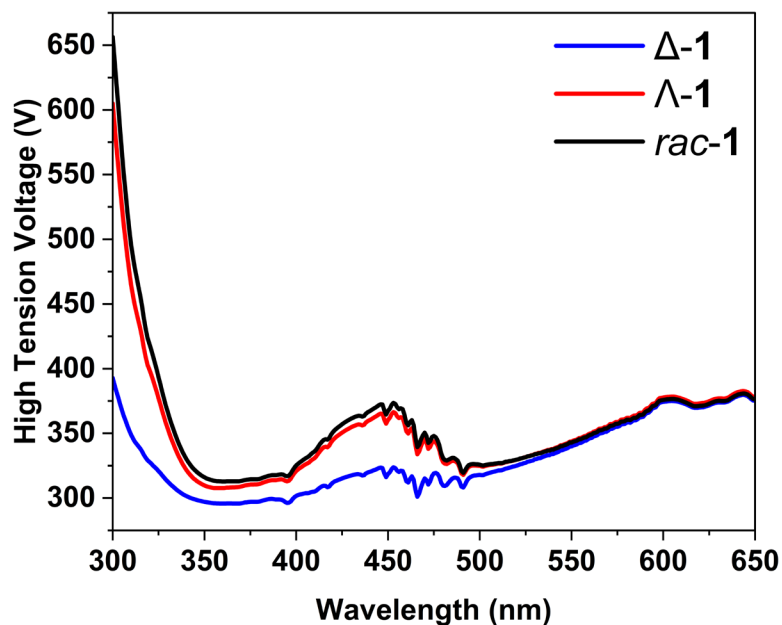
Figure S24: High tension (HT) voltage profiles for each sample.
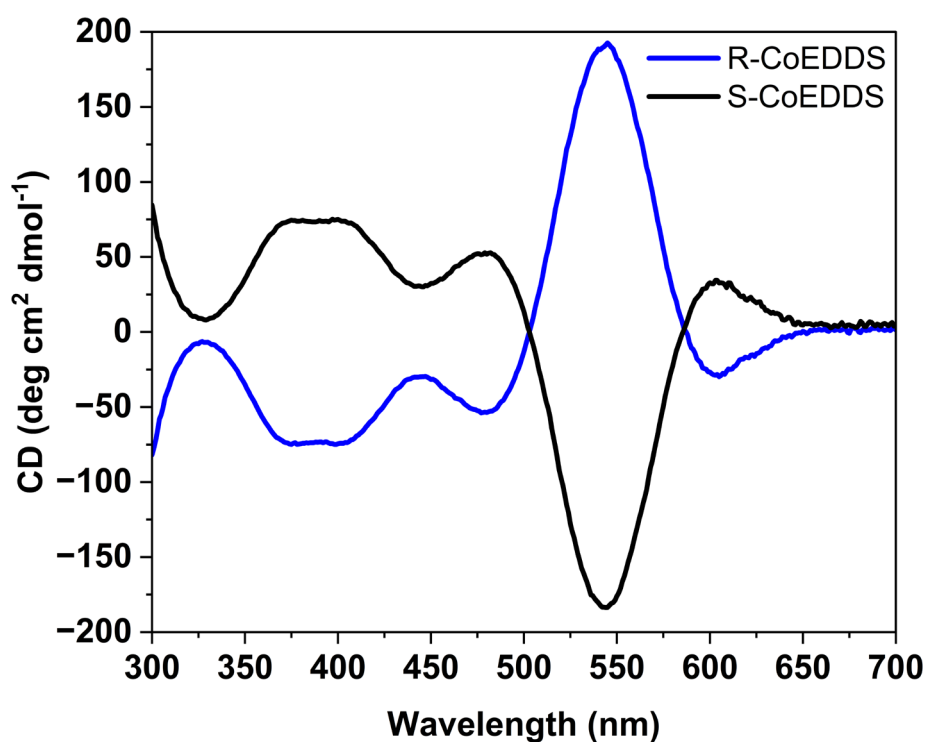
Figure S25: Circular dichroism (CD) spectra of the standard *R*- and *S*-Co^{III} EDDS (where, EDDS = ethylenediamine-*N,N'*-disuccinic acid) solutions in water used to calibrate the instrument prior to sample measurement. Each solution was run between 300-700 nm using a 1 cm quartz cell for a single accumulation.

SEM-EDS

Figure S26: SEM micrographs and EDS spot analysis of (a) Δ-**1**, (b) Λ-**1**, and (c) *rac*-**1**.

PXRD

Bulk samples of each helicate were ground and layered onto separate low background silicon XRD plates coated with a small layer of amorphous grease to fix the crystallites into position. All data processing was cond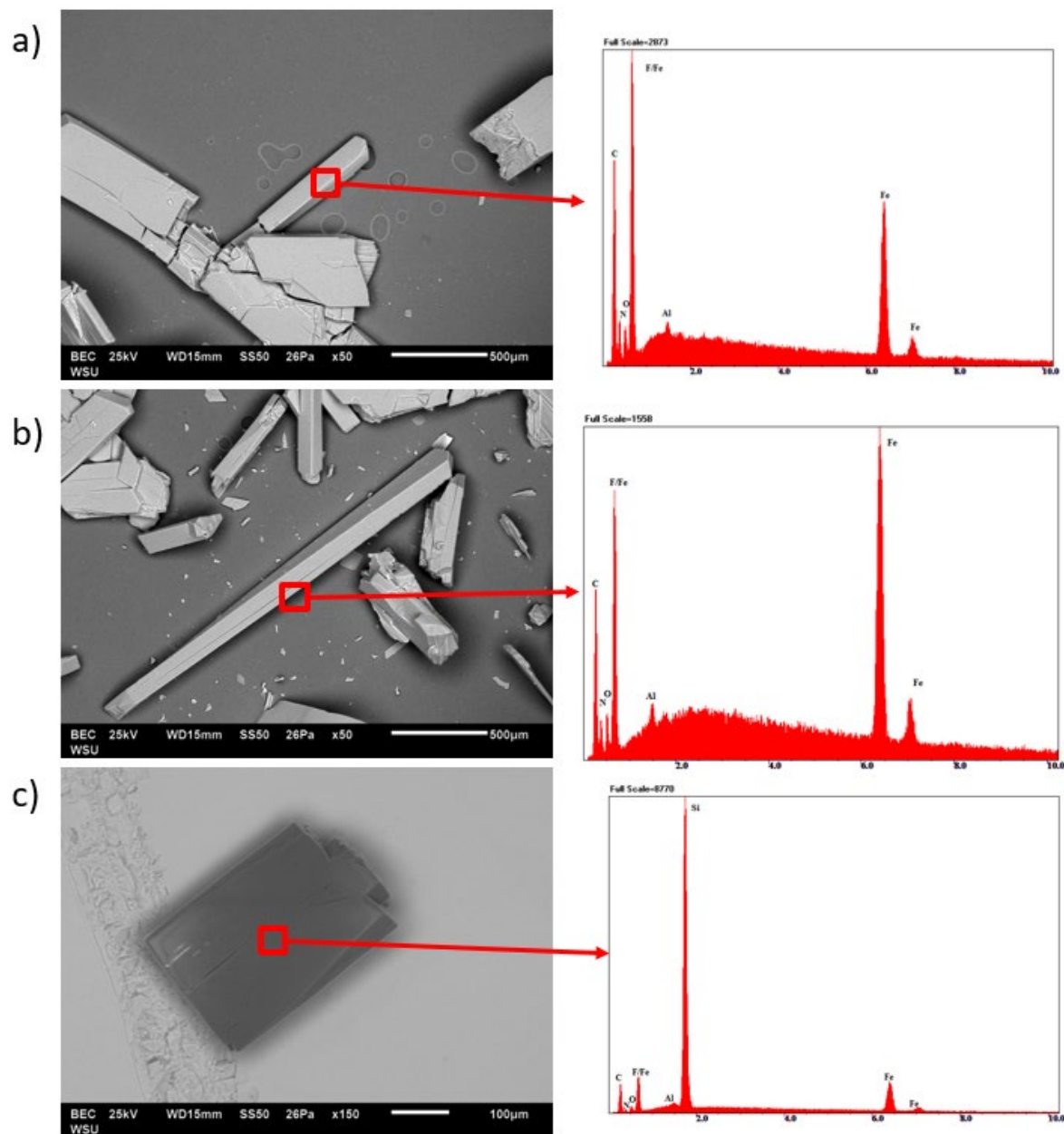ucted using Bruker's EVA software. Data refinement of each helicate was performed on the unit cell parameters obtained from the CIFs generated from SC-XRD measurements and fitted against the experimental powder pattern using a Pawley refinement in TOPAS v6. The fit of each helicate demonstrates that the bulk material is homogeneous to the single crystal sample.

Figure S27: Pawley refinement of the experimental and simulated powder pattern of Δ-**1** obtained at room temperature. The simulated (red) and experimental (blue) powder patterns are shown above the difference (grey). The experimental pattern was collected using a CuKα1 source (1.5406 Å). GOF = 4.15, Rexp = 3.61, Rwp = 15.01, Rp = 10.51.

Figure S28: Pawley refinement of the experimental and simulated powder pattern of Λ-**1** obtained at room temperature. The simulated (red) and experimental (blue) powder patterns are shown above the difference (grey). The experimental pattern was collected using a CuKα1 source (1.5406 Å). GOF = 4.58, Rexp = 3.95, Rwp = 18.10, Rp = 12.15.
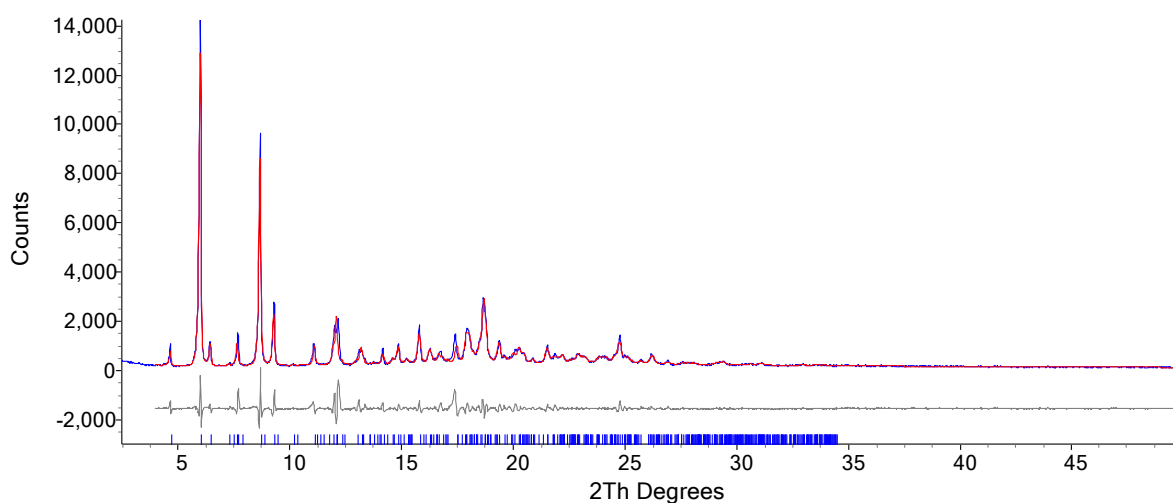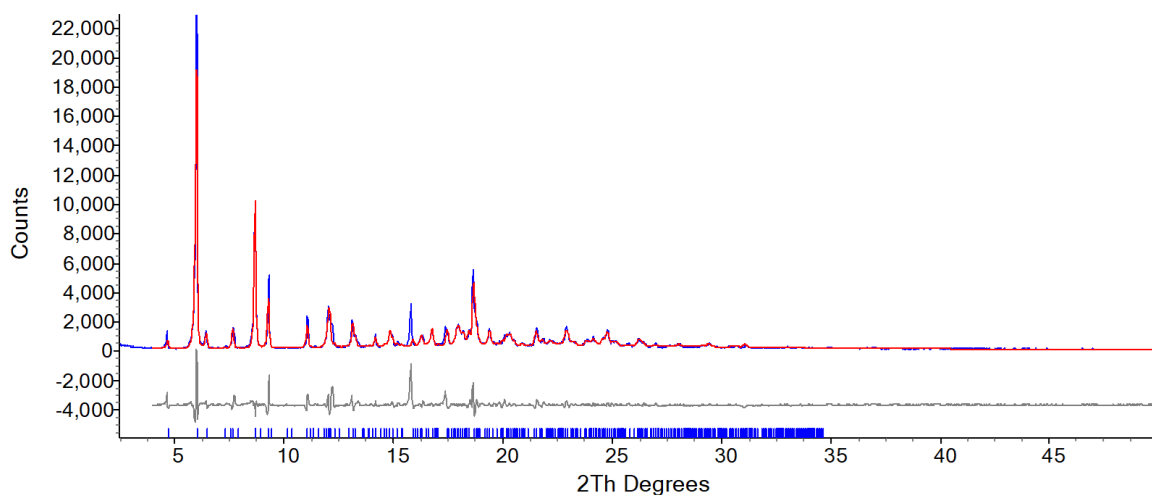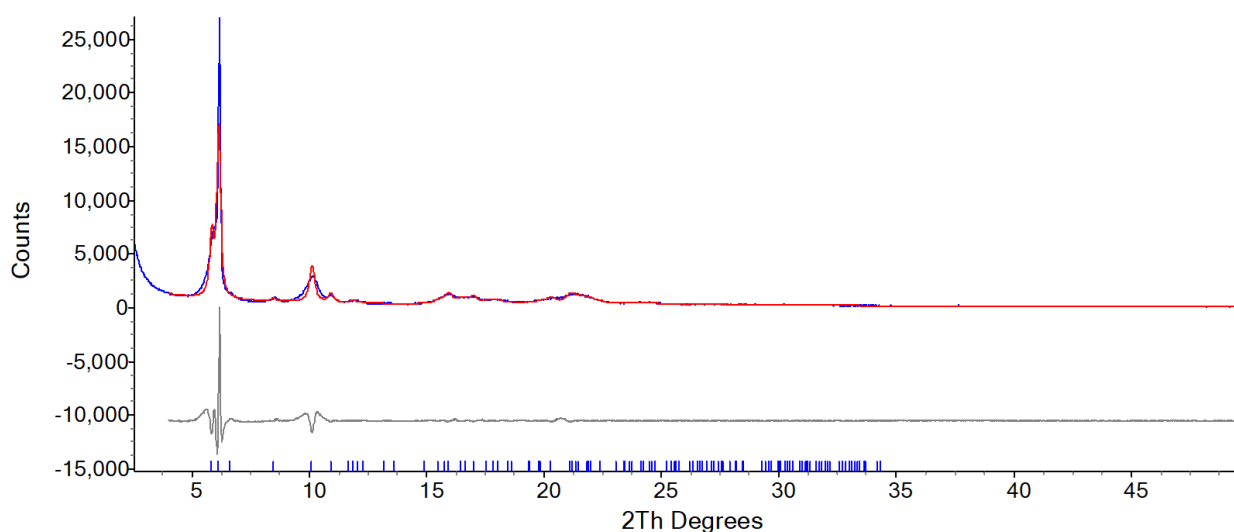

Figure S29: Pawley refinement of the experimental and simulated powder pattern of *rac*-**1** obtained at room temperature. The simulated (red) and experimental (blue) powder patterns are shown above the difference (grey). The experimental pattern was collected using a CuKα1 source (1.5406 Å). GOF = 3.97, Rexp = 4.13, Rwp = 16.42, Rp = 11.71.

TGA-DSC

Figure S30: TGA-DSC for Δ-**1** over the temperature range 300-860 K at a scan rate of 10 K min⁻¹.

Figure S31: TGA-DSC for Λ-**1** over the temperature range 300-860 K at a scan rate of 10 K min⁻¹.

Figure S32: TGA-DSC for *rac*-**1** over the temperature range 300-860 K at a scan rate of 10 K min⁻¹.

Crystallographic Information

Table S1: Crystallographic parameters for Δ-**1**, Λ-**1**, and *rac*-**1**.

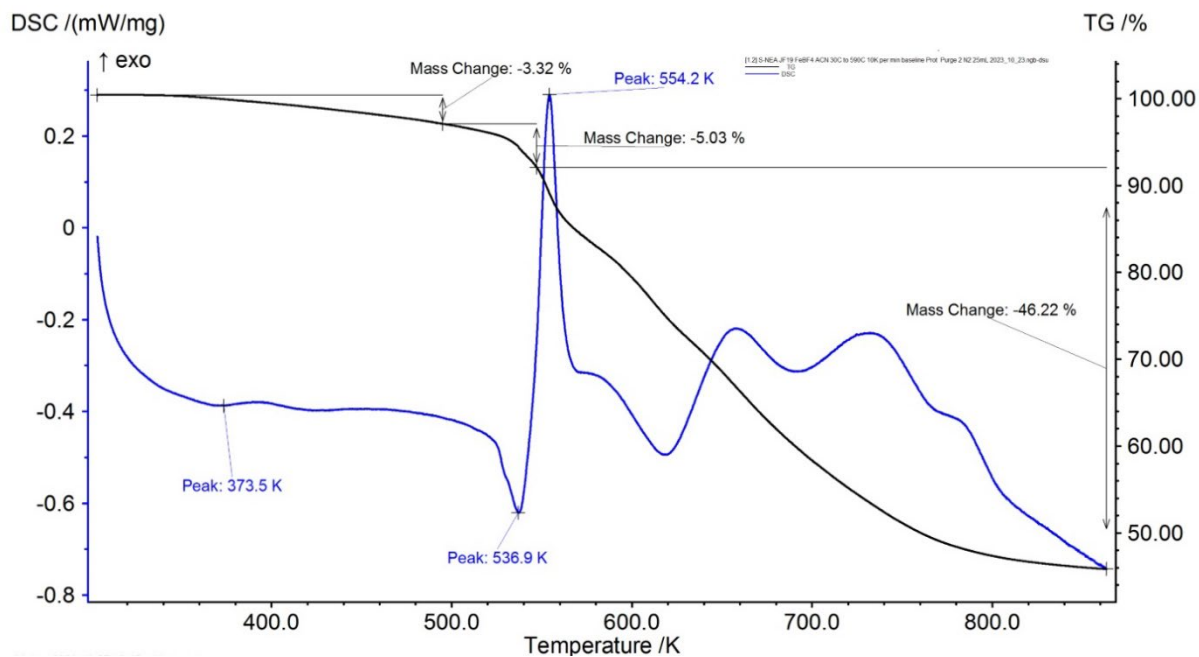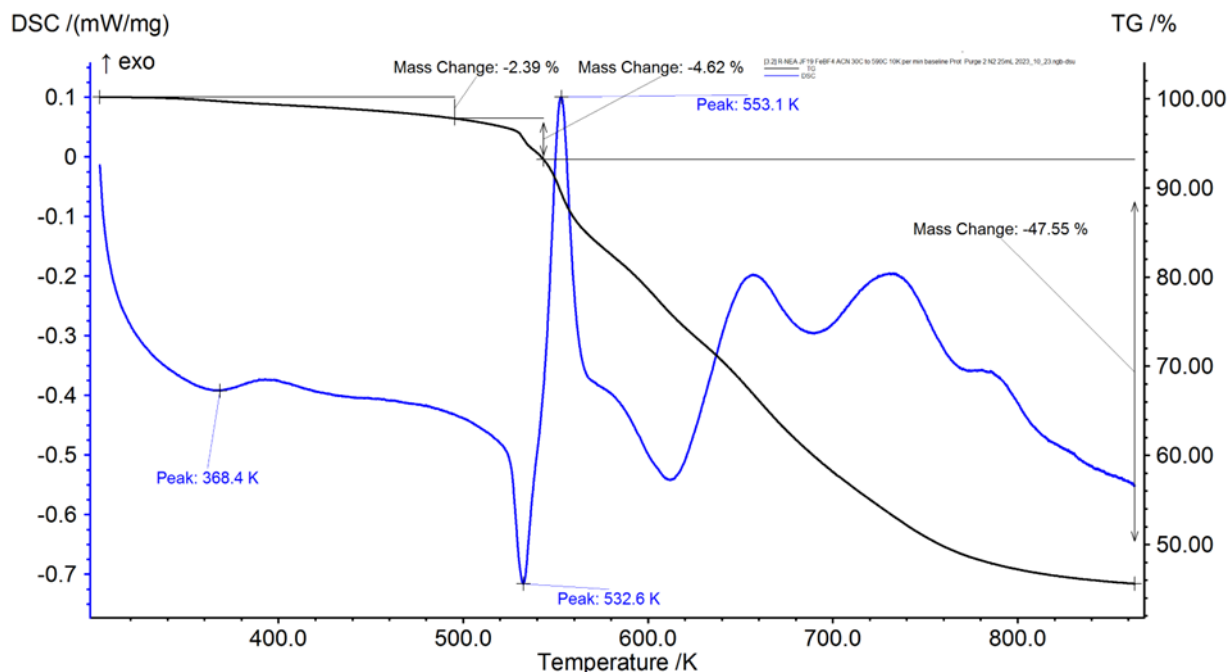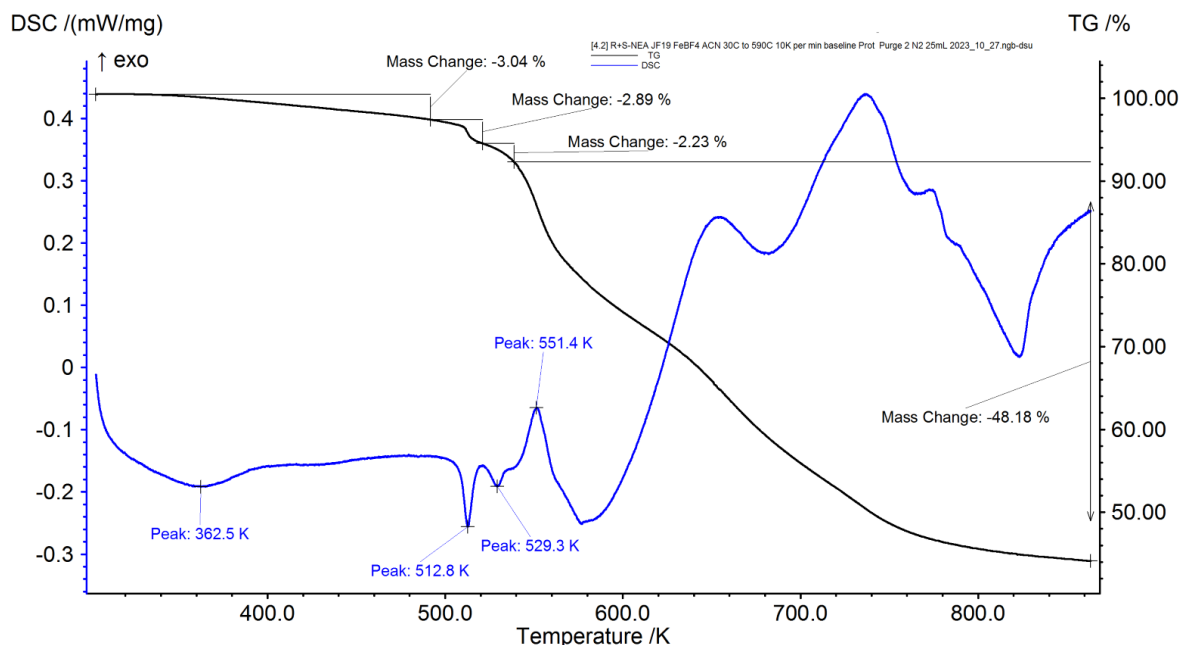| Compound	Δ-**1**		Λ-**1**		*rac*-**1**	
Temperature (K)	100	300	100	300	100	300
Empirical formula	$C_{152}H_{152}B_4F_{16}Fe_2N_{30}O_2$	$C_{138}H_{125}B_{3.85}F_{16.08}Fe_2N_{25}O$	$C_{140.35}H_{114}B_4F_{16}Fe_2N_{24.94}O_2$	$C_{136.04}H_{127.56}B_4H_{16.5}Fe_2N_{24}O_{0.92}$	$C_{132}H_{148}B_4F_{16}Fe_2N_{24}O_{20}$	$C_{132}H_{126}B_7F_{44}Fe_2N_{24}O_6$
Formula weight	2889.97	2608.50	2640.80	2581.89	2849.68	3167.93
Temperature/ K	100	300	100	300	100	300
Crystal system	Monoclinic	Monoclinic	Monoclinic	Monoclinic	Trigonal	Trigonal
Space group	$P2_1$	$P2_1$	$P2_1$	$P2_1$	P-31c	P-31c
a/Å	13.043(3)	13.110(3)	13.030(3)	13.090(3)	17.524(3)	17.924(3)
b/Å	37.961(8)	37.380(8)	37.450(8)	37.530(8)	17.524(3)	17.924(3)
c/Å	15.795(3)	15.630(3)	15.720(3)	15.590(3)	28.840(6)	28.938(6)
α/°	90	90	90	90	90	90
β/°	111.88(3)	111.99(3)	112.56(3)	111.49(3)	90	90
γ/°	90	90	90	90	120	120
Volume/Å³	7257(3)	7102(3)	7084(3)	7126(3)	7670(3)	8051(3)
Z	2	2	2	2	2	2
$\rho_{calc}g/cm^3$	1.323	1.220	1.238	1.203	1.234	1.307
μ/mm^{-1}	0.285	0.282	0.284	0.281	0.275	0.287
F(000)	3012.0	2704.0	2725.0	2679.0	2968.0	3234.0
Crystal size/mm³	0.1x0.1x0.1	0.1x0.1x0.1	0.1x0.1x0.1	0.1x0.1x0.1	0.1x0.1x0.1	0.1x0.1x0.1
Radiation	MoKα (λ = 0.71073)	MoKα (λ = 0.71073)	MoKα (λ = 0.71073)	MoKα (λ = 0.71073)	MoKα (λ = 0.71073)	MoKα (λ = 0.71073)
2Θ range for data collection/°	2.146 to 49.428	2.178 to 53.008	2.174 to 57.294	2.17 to 52.744	2.684 to 50.036	2.978 to 54.958
Index ranges	$-15 \le h \le 14, -43 \le k \le 43, -18 \le l \le 18$	$-15 \le h \le 16, -45 \le k \le 46, -19 \le l \le 19$	$-17 \le h \le 17, -50 \le k \le 49, -21 \le l \le 20$	$-16 \le h \le 16, -46 \le k \le 46, -19 \le l \le 19$	$-20 \le h \le 20, -20 \le k \le 20, -30 \le l \le 32$	$-20 \le h \le 20, -20 \le k \le 20, -30 \le l \le 31$

| Reflections collected	81976	208364	181255	175421	85774	98890
Independent reflections	23084 [R_{int} = 0.0227, R_{sigma} = 0.0193]	25256 [R_{int} = 0.0510, R_{sigma} = 0.0305]	31268 [R_{int} = 0.0455, R_{sigma} = 0.0302]	28486 [R_{int} = 0.1085, R_{sigma} = 0.0666]	4413 [R_{int} = 0.0308, R_{sigma} = 0.0083]	5313 [R_{int} = 0.0302, R_{sigma} = 0.0112]
Data/restrains/parameters	23084/1069/2093	25256/213/1690	31268/392/1743	28486/487/1664	4413/73/321	5313/39/299
Goodness-of-fit on F^2	1.038	1.039	1.113	0.983	1.685	1.748
Final R indexes [I>=2σ (I)]	R_1 = 0.0663, wR_2 = 0.1867	R_1 = 0.0928, wR_2 = 0.2437	R_1 = 0.0882, wR_2 = 0.2453	R_1 = 0.0850, wR_2 = 0.2148	R_1 = 0.1171, wR_2 = 0.3661	R_1 = 0.1198, wR_2 = 0.3586
Final R indexes [all data]	R_1 = 0.0670, wR_2 = 0.1881	R_1 = 0.1355, wR_2 = 0.2830	R_1 = 0.0994, wR_2 = 0.2615	R_1 = 0.1335, wR_2 = 0.2478	R_1 = 0.1254, wR_2 = 0.3805	R_1 = 0.1261, wR_2 = 0.3742
Largest diff. peak/hole / e $Å^{-3}$	0.89/-0.51	0.80/-0.29	1.88/-0.65	0.99/-0.45	1.03/-0.46	1.47/-0.90
Flack parameter	0.019(3)	0.026(5)	0.031(4)	0.012(7)	-	-

Hirshfeld Isosurfaces
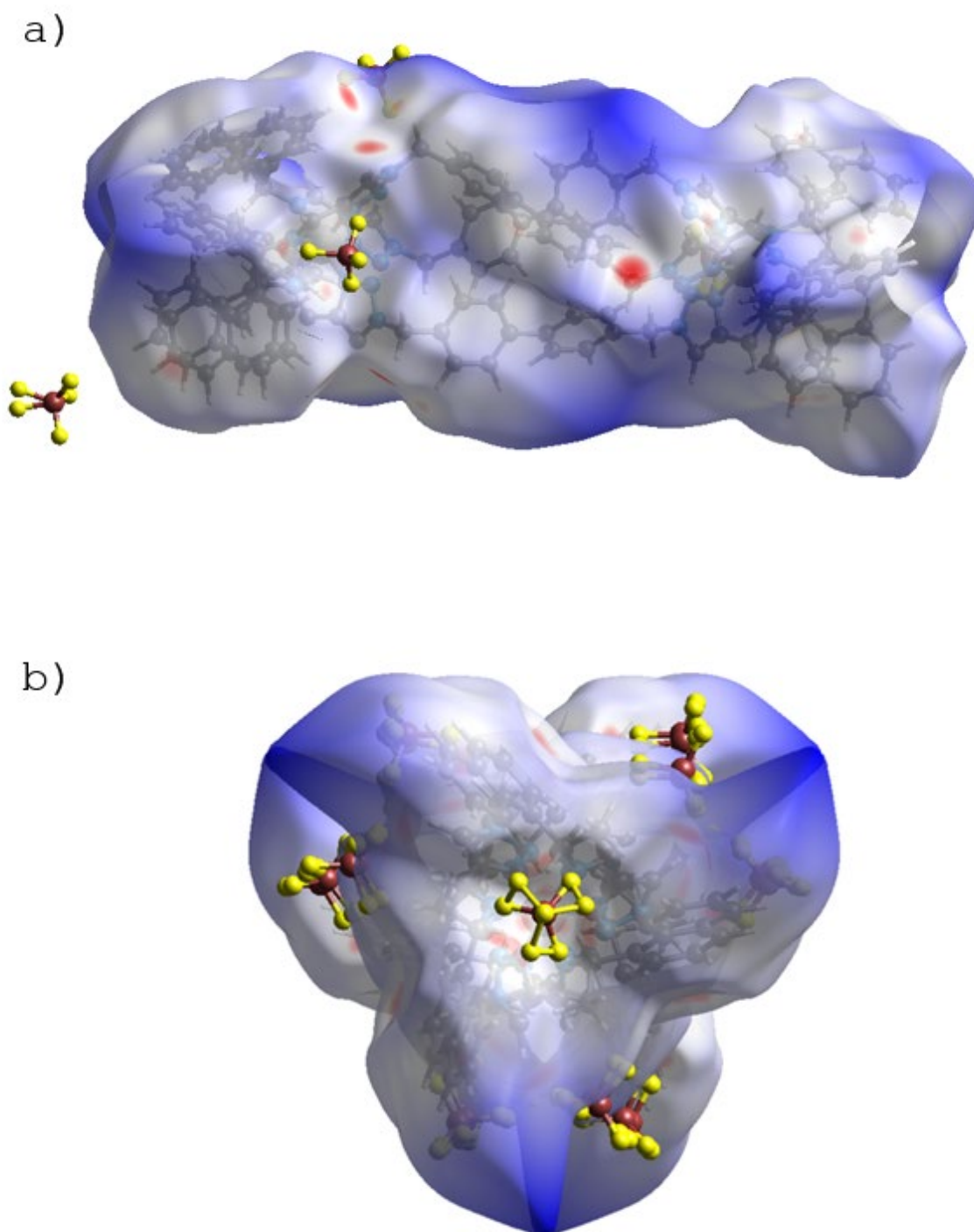
Figure S34: Hirshfeld surfaces for (a) Λ-**1** and (b) an alternate view of *rac*-**1**.

References

1. Thomas, J. R.; Liu, X.; Hergenrother, P. J. Size-Specific Ligands for RNA Hairpin Loops. *J. Am. Chem. Soc.* **2005**, *127* (36), 12434–12435. https://doi.org/10.1021/ja051685b.